Role of the RNA binding protein Musashi2 in myogenesis

２０２２

王　　若冲

Contents

Summary

Understanding the regulatory mechanisms of skeletal muscle development and function is vital for keeping and improving human health. Past studies have identified myogenic regulatory factors (MRFs) regulate a cascade of genes for skeletal muscle development at the transcriptional level. Recent studies also discovered that RNA binding proteins (RBPs) play essential roles in the post-transcriptional regulation of myogenesis.

The RBP Musashi2 (Msi2) is a translational regulator of cell fates in normal tissues such as hematopoietic, mammary, and neural tissues, as well as in cancers, including glioblastoma and leukemia. Msi2 is also expressed in normal skeletal muscle tissues, but its role in myogenesis remains largely unknown. This thesis aims to comprehensively understand how Msi2 regulates skeletal muscle development and function.

In order to assess the importance of Msi2 in myogenic differentiation, I utilized the C2C12 mouse myoblast cell line as a model. First, I analyzed Msi2 expression during C2C12 differentiation and found that Msi2 is greatly upregulated during the differentiation process. In contrast to a well-characterized role of Msi2 in stemness in hematopoietic or neural lineages, Msi2 is likely to be functional as a differentiation factor in myoblast. Next, to examine if Msi2 is required for this process, I performed knockdown (KD) of Msi2 expression by a lentiviral short hairpin RNA interference method. In the control cells, I observed mature myotubes with multiple nuclei and myosin heavy chain (MHC) by immunofluorescence staining at 5 days after differentiation induction. In contrast, Msi2-KD cells showed very few MHC-positive cells in which 1 or 2 nuclei were detected. This result suggests that Msi2 is required for myocyte differentiation and fusion process, which is necessary for mature myotube formation. Interestingly, the protein or mRNA

level of Myogenin, an essential MRF that controls MHC expression and terminal differentiation, is not changed by Msi2 KD, suggesting that Msi2 does not regulate the canonical MRF network. Overexpression (OE) of Msi2 successfully rescued the impaired differentiation phenotypes observed in the KD cells, which excluded the possibility of an off-target effect of the Msi2-KD construct. Surprisingly, I noticed that Msi2 OE alone generated thicker and longer myotubes 5 days after expression. These results suggest that Msi2 promoted myocyte differentiation and fusion, and is not only necessary but also sufficient for myoblast differentiation.

As a molecular mechanism of myocyte differentiation by Msi2, I hypothesized that Msi2 regulates mitochondrial function and biogenesis, which are critical factors in myogenesis. Using MitoTracker Deep Red, an indicator of functional mitochondria, I found the staining level is lower in Msi2-KD cells and higher in Msi2 OE cells compared to the control. I also found that mitochondrial DNA content and mitochondrial respiration function measured by the Seahorse assay were comparable between the control and KD. Since staining with MitoTracker Deep Red is dependent on mitochondrial membrane potential ($\Delta\Psi m$), these results suggest that Msi2 regulates $\Delta\Psi m$ without affecting mitochondrial biogenesis. Next, I examined if Msi2 regulates autophagy during myoblast differentiation because changes in $\Delta\Psi m$ can both trigger and be regulated by autophagy. First, I found that the level of autophagosome marker LC3A-II correlates with the Msi2 expression level during C2C12 differentiation. Msi2 KD reduced both the LC3A-II level and formation of LC3A-positive puncta, suggesting that Msi2 KD impairs autophagy during myoblast differentiation. To further test if differentiation defects caused by Msi2 KD are autophagy-dependent, I induced autophagy in control or Msi2-KD cells by using Tat-Beclin1-D11, which is a short peptide that can upregulate autophagy through binding to the autophagy suppressor GAPR-1/GLIPR2. Strikingly, the Tat-Beclin1-D11 treatment

significantly increased myocyte differentiation and fusion levels in Msi2-KD cells, indicating the Msi2-KD phenotype can be rescued by activation of autophagy.

To examine the function of Msi2 in skeletal muscle in vivo, I used a Msi2 mutant mouse strain generated by a germline gene-trap strategy. The hind limb muscles of Msi2 mutant mice are also smaller in size and paler in color than wild-type controls (WT). In a treadmill exercise assay, Msi2 mutant mice could run only 30 meters on average, compared to more than 100 meters for WT mice. These results suggest that Msi2 mutant mice have defective skeletal muscle.

In conclusion, this thesis study has established that Msi2 is a novel regulator of skeletal muscle development and function by regulating autophagy and provided insights for future studies on the role of Msi2 in cancer metabolism and myopathies.

Introduction

Skeletal muscle is vital for body movement, energy expenditure and metabolism. Skeletal muscle formation is a highly ordered process named myogenesis[1]. In adulthood, myogenesis process is initiated by the differentiation of satellite cells, which are muscle stem cells, into the muscle progenitors myoblasts, while maintaining the stem cell population at the same time through asymmetric cell division[2]. Myoblasts will further proliferate and terminally differentiate into mature myocytes, and fuse with each other into multi-nucleated myotubes and eventually form functional myofibers[3]. To date, the regulation of myoblast differentiation is well characterized at the transcriptional level. This process is mainly controlled by a family of transcription factors named the myogenic regulatory factors (MRFs), including MyoD, Myf5, Myogenin, and MRF4[4,5]. However, how myogenesis is regulated besides transcription regulation is not fully understood.

Autophagy, which is the major intracellular degradation system, plays vital roles in cell renovation and homeostasis[6]. Since muscle is highly metabolically active tissue and requires metabolic reprogramming, recent findings have suggested autophagy as an essential element for normal myogenesis [7–9]. In skeletal muscle, autophagy helps maintain healthy and functional muscles while deficiency in autophagy will lead to muscle atrophy[10–13]. In contrast, hyper activation of autophagy can also be observed in dystrophic muscles under cachexia and aging[14,15]. These findings suggest a highly dynamic and tightly regulated role of autophagy in skeletal muscle development.

Recent studies showed that RNA-binding proteins (RBPs) are crucial factors for the post-transcriptional regulation of myogenesis as well[16]. RBPs can bind to mRNAs and regulate their splicing, modification, stability, and translation[17]. In mouse, hundreds of RBPs are predicted to be expressed in skeletal muscle. However, only a very small proportion of these RBPs have been studied[18], suggesting a huge gap of knowledge of

how RBPs regulate skeletal muscle development and function at the post-transcriptional level. Recent studies showed that a variety of RBPs can regulate the myogenesis through binding with muscle differentiation genes, including HuR[19], KSRP[20], and hnRNPL[21]. Still, how myogenesis is regulated at post-transcriptional level has not been fully studied.

The Musashi family of RBPs are well known for regulating stem cell maintenance and cell fate decision[22]. In mammalian species, there are two members in the family, Musashi-1 (Msi1) and Musashi-2 (Msi2). Mouse Msi1 and Msi2 have a similar overall structure with 75% amino acid identity. Both have two highly conserved RNA recognition motifs (RRMs), RRM1 and RRM2, for binding to specific RNA targets[23]. Msi1 but not Msi2 also contains a C-terminal domain that has been shown to bind the poly (A)-binding protein (PABP)[24]. Msi1 has been extensively studied for its function in stem cells of various tissues as well as in cancers, such as normal brain and intestine, breast cancer, and colon cancer[25–28]. Though Msi2 shows an overlapping expression pattern with Msi1, Msi2 is specifically expressed and functions as a critical translational regulator of cell fates in normal hematopoietic stem cell[29,30], as well as in many cancers, including leukemia, breast cancer, and non-small cell lung cancer[31–34]. Besides the central nervous and hematopoietic systems, Msi2 is also highly expressed in normal skeletal muscles. However, its role in myogenesis remains largely unknown. Other than translational regulation, a recent study suggests the possibility that Msi2 regulates autophagy by direct binding with the Beclin1 protein, an autophagy mediator, in malignant peripheral nerve sheath tumors[35,36]. However, the relationship between Msi2 and autophagy has barely been studied.

In this study, I addressed these issues *in vitro* using the C2C12 mouse myoblast cell line, which is a widely used model for studying myogenic differentiation[37–39], and *in vivo* using Msi2 gene-trap mutant mice. Surprisingly, Msi2 was found to be essential for

the differentiation and fusion of C2C12 cells, via promoting autophagy during the process. On the other hand, the Msi2 mutant mice exhibited smaller and weaker skeletal muscles. These findings in this study identify Msi2 as a novel regulator of myogenesis and autophagy, which provide new insights into our understanding of muscle development and the relationship between autophagy and myogenesis.

Results

Msi2 expression during myoblast differentiation

In order to examine the contribution of Msi2 in muscle development, first I analyzed its expression during myocyte differentiation in the C2C12 mouse myoblast cell line, which is a well characterized in vitro model for studying myogenesis process[37]. In a fetal bovine serum-based media (Growth Media or GM), C2C12 cells expand themselves as myoblasts. The cells undergo myocyte differentiation after placing them in a media with a donor equine serum (Differentiation Media or DM), and within 5 days these myocytes form multi-nucleated myotubes (Fig. 1A). I found that the expression of Msi2 protein was upregulated soon after the induction of myocyte differentiation by DM (Figs. 1B and C). Immunofluorescence staining of the Msi2 protein confirmed its upregulation upon differentiation induction (Fig. 1D). Interestingly, C2C12 cells exhibited heterogeneity in the levels of Msi2 protein, and cells with higher Msi2 expression showed more differentiated morphology with more nuclear Msi2 staining at Days 3 and 6 after differentiation induction. Upregulation of Msi2 was concomitant with Myogenin (Myog), followed by the induction of myosin heavy chain (MHC; Fig. 1B), which is a marker for mature myocytes. Myog is an E-box transcription factor essential for myocyte differentiation and regulates several myocyte-specific genes, including MHCs[40,41]. Msi1, the other member of the mammalian Msi RBP family, was not expressed or upregulated during C2C12 differentiation. The anti-Msi1 antibody was validated using control and *Msi1* knockout (*Msi1*-KO) mouse brain samples (Fig. 1E). Taken together, these results suggested that Msi2 but not Msi1 may have specific roles in myocyte differentiation

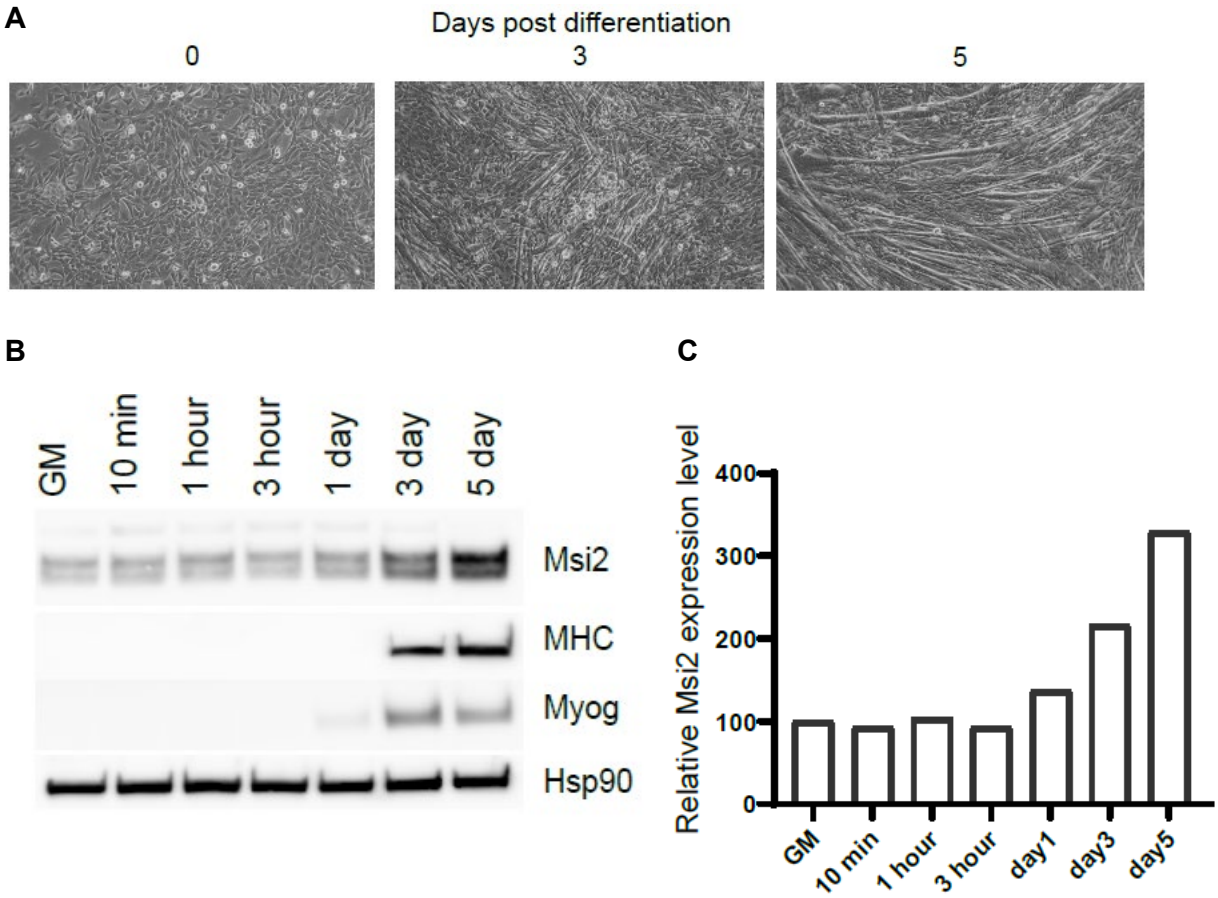
A
Days post differentiation
0
3
5
B
GM
10 min
1 hour
3 hour
1 day
3 day
5 day
Msi2
MHC
Myog
Hsp90
C
Relative Msi2 expression level
400
300
200
100
0
GM
10 min
1 hour
3 hour
day1
day3
day5
D
Anti-Msi2
Normal IgG
Days post differentiation
0
3
6
0
Msi2
Nucleus
Overlay

E

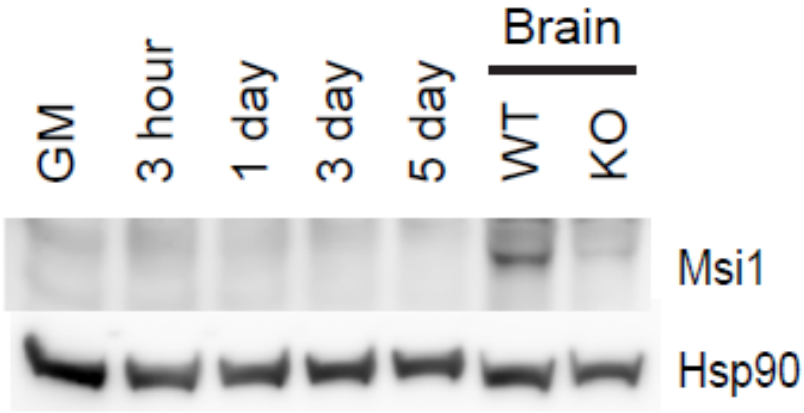

Fig. 1. Upregulated Msi2 expression during C2C12 differentiation.

A. Phase-contrast images of the C2C12 cells during differentiation.

B. Western blotting (WB) analysis of Msi2 protein expression during C2C12 differentiation. Protein samples were collected at different time points after differentiation induction. MHC and Myogenin were used as differentiation markers. HSP90 was used as a loading control. GM means the sample in growth media.

C. Relative Msi2 expression level normalized to the Hsp90 loading control. The Msi2 level at non-differentiation time point was set as 100.

D. Confocal microscopy of C2C12 with IF staining of Msi2 and DAPI staining at different differentiation stage. Normal IgG was used as a negative control. Images were taken under 63x lens.

E. WB analysis of Msi1 protein expression during C2C12 differentiation. Protein samples were collected at different time points after differentiation induction. Hsp90 was used as a loading control. Brain samples collected from WT and *Msi1*-KO mice were used as positive and negative controls for the Msi1 protein.

Msi2 is essential for the terminal differentiation of myocytes

Next, I investigated whether Msi2 is functionally required for myocyte differentiation by using lentiviral short hairpin RNA (shRNA)-mediated gene KD approach. After 3 days of the viral transfer of an shRNA against mouse Msi2 (shMsi2), the cells showed no detectable Msi2 protein expression and that the effect of the KD continued up to 7 days (Fig. 2A, Msi2). In the Growth Media, shMsi2-expressing cells proliferate as much as those with a control shRNA (shLuc) does, indicating Msi2 is not essential for cell growth or survival (Fig. 2B). After differentiation induction, the control cells started to show elongated myotubes at as early as 3 days post differentiation induction (Fig. 2C, shLuc). The cells expressing shMsi2 also generated elongated cells, but they appeared shorter in length and their numbers were much less than those with shLuc even after 5 days of differentiation, indicating a significant impairment of myotube formation in the absence of Msi2 (Fig. 2C, shMsi2). The MHC protein was upregulated in shMsi2 cells, but the magnitude of expression induction was not as robust as that of shLuc cells (Figs. 2A). In contrast, the Myog level was comparable between the control and the Msi2-KD cells, suggesting the lower MHC induction is not due to a defect in Myog expression (Figs. 2A, Myog).

To address whether the differentiation is impaired at a specific stage during myotube formation, I monitored differentiation status using immunofluorescence microscopy. Consistent with the phase contrast images shown in Fig. 3C, after 5 days of differentiation, the shLuc control cells generated MHC-positive elongated myotubes while the Msi2-KD cells generate much less and smaller MHC-positive cells (Fig. 2D). I observed some elongated cells in shMsi2 cells, but interestingly, most of them were GFP-negative, indicating that these mature myocytes are not expressing shMsi2 (Fig. 2D, arrows). The ratio of nuclei in MHC-positive cells by total nuclei in the shRNA-expressing GFP+ cells, *i.e.,* the differentiation index, was significantly lower in the shMsi2

group than in the control group (Fig. 2E). In addition, the shMsi2 cells exhibited a much lower fusion index, defined as the number of myonuclei in one MHC^+ cell, indicating an impact of Msi2 KD on the myocyte fusion step (Fig. 2F).

Consistent with the immunostaining of MHC proteins, mRNA analysis of mouse myosin heavy chain genes *MYH1* and *MYH4* confirmed their attenuated expressions by the Msi2 KD (Fig. 2G). In contrast, the *Myod1* and *Myog* expression levels were comparable in both groups, suggesting the decreased MHC gene expressions in the Msi2 KD are downstream or independent of the transcriptional regulation by the myogenic transcription factors Myod1 and Myog (Fig. 2G). Collectively, these data demonstrated an essential role of Msi2 in the terminal differentiation of myocytes.

A

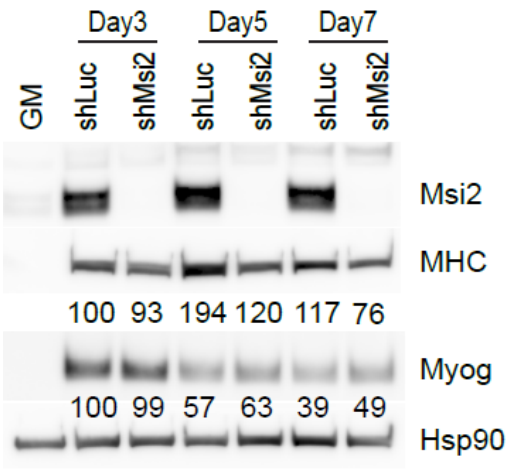
Day3
Day5
Day7
GM
shLuc
shMsi2
shLuc
shMsi2
shLuc
shMsi2
Msi2
MHC
100 93 194 120 117 76
Myog
100 99 57 63 39 49
Hsp90

B

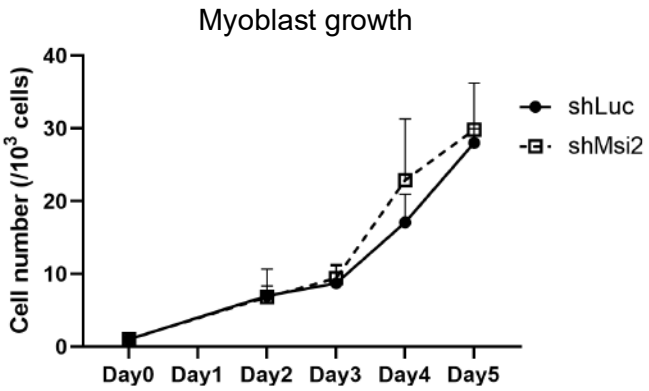
Myoblast growth
Cell number (/10^3 cells)
40
30
20
10
0
Day0 Day1 Day2 Day3 Day4 Day5
shLuc
shMsi2

C

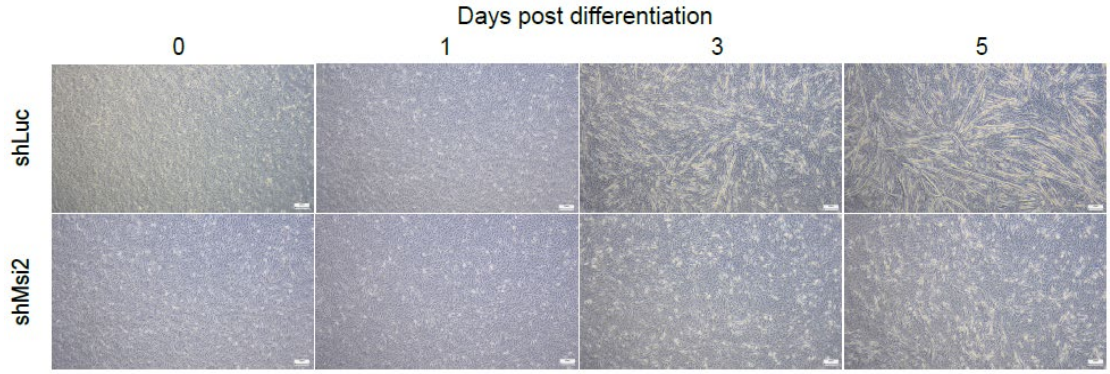
Days post differentiation
0
1
3
5
shLuc
shMsi2

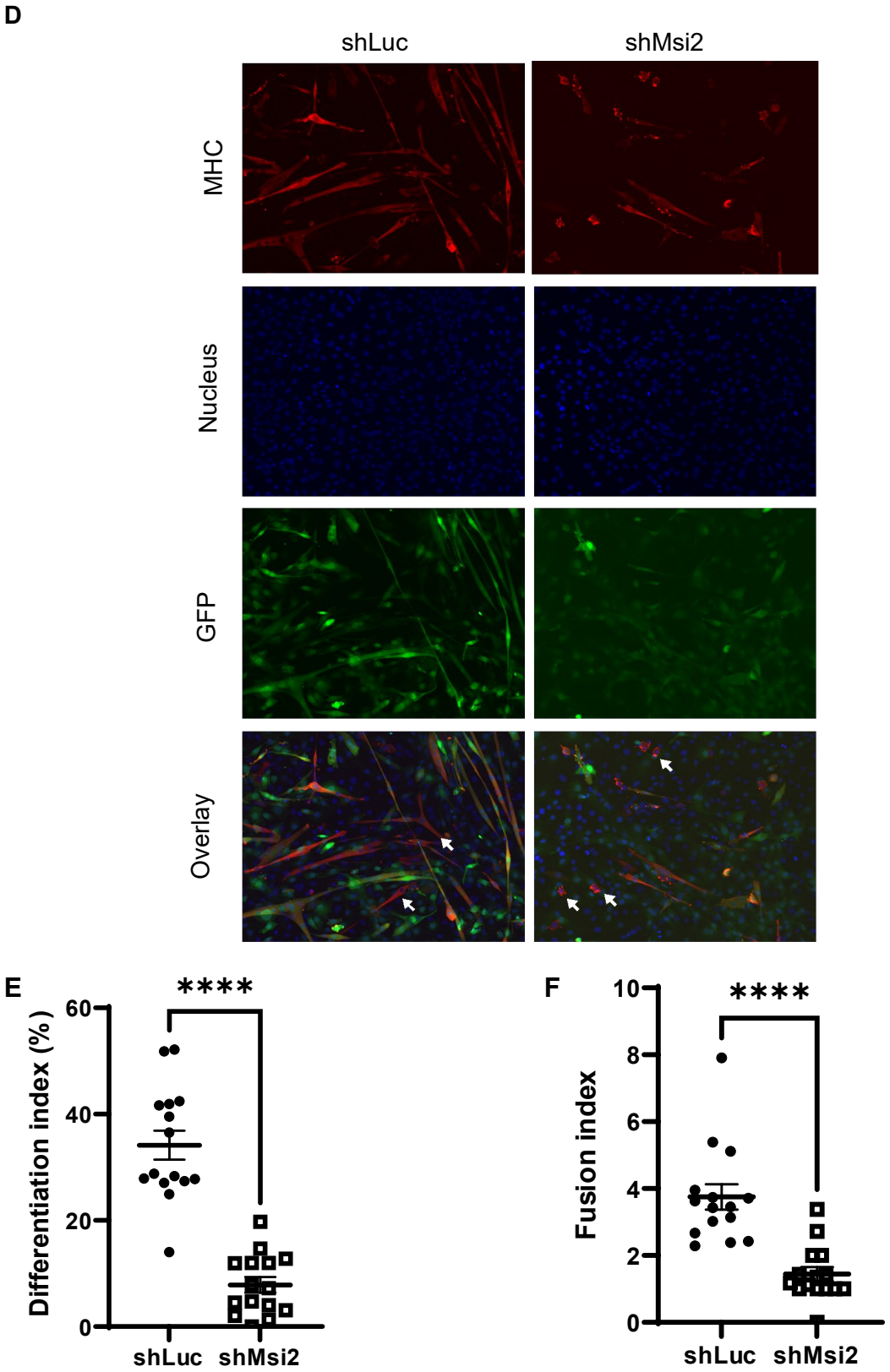
D
shLuc
shMsi2
MHC
Nucleus
GFP
Overlay
E
****
Differentiation index (%)
60
40
20
0
shLuc
shMsi2
F
****
Fusion index
10
8
6
4
2
0
shLuc
shMsi2

G

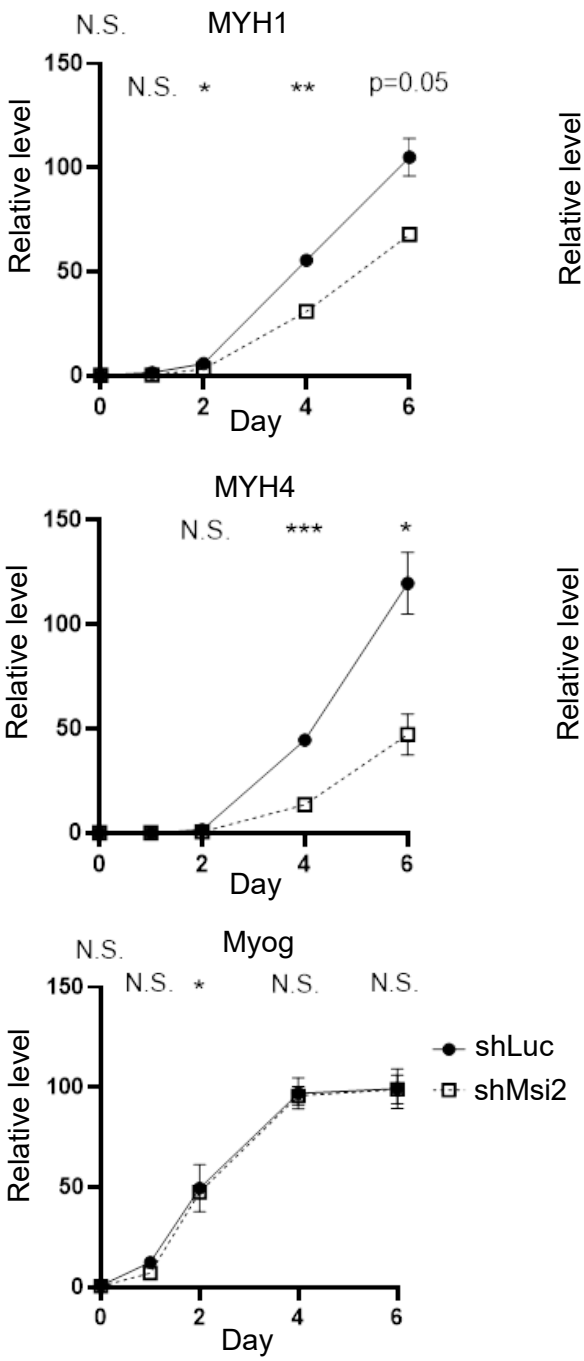
MYH1
N.S.
N.S.
*
**
p=0.05
Relative level
Day
MYH3
N.S.
*
N.S.
*
N.S.
MYH4
N.S.
***
*
Myod1
N.S.
*
N.S.
N.S.
N.S
Myog
N.S.
N.S.
*
N.S.
N.S.
shLuc
shMsi2

Fig. 2. Msi2 KD impairs C2C12 differentiation.

A. Effects of the Msi2 KD on C2C12 differentiation. C2C12 cells treated with lentiviral shLuc control or shMsi2 were collected at different time points after differentiation induction. The very top bands shown in all samples in Msi2 WB is non-specific bands. Numbers below the bands are densitometric analysis results normalized to those of Hsp90 loading control.

B. Growth curve analysis of lentiviral shLuc or shMsi2 treated C2C12 cells in growth media (GM). Two individual experiments with 2 replicates in each group are combined.

C. Phase contrast images of lentiviral shLuc- or shMsi2-transduced C2C12 cells during differentiation.

D. Immunofluorescence staining of MHC in lentiviral shLuc or shMsi2 transduced C2C12 cells on day6 after differentiation induction. MHC was stained to show differentiated myocytes. GFP positive cells are virus transfected. DAPI was used to stain nucleus. Non-infected MHC+ cells are pointed out by white arrows.

E, F. Quantification of the differentiation index (**E**) and fusion index (**F**) for the C2C12 cells on day 6 after differentiation induction. Each dot represents one field taken as shown in panel E. Five fields were picked in each experiment. Data from three independent experiments were combined. Unpaired *t*-test was performed between the shLuc and shMsi2 groups.

G. RT-qPCR analysis of *MYH1, MYH3, MYH4, Myog* and *Myod1* expression in C2C12 cells transduced with the lentiviral shLuc or shMsi2 vector. The expression levels are normalized to the expression level of b2M, beta-2-macroglobulin. Un-paired *t*-test was used to compare relative mRNA level from each time points between the shLuc and shMsi2 groups.

Msi2 expression rescues the differentiation defects conferred by the shMsi2

To exclude a possibility of an off-target effect by the lentiviral shMsi2 and further confirm the functional requirement of Msi2 in myoblast differentiation, I investigated if Msi2 overexpression can rescue the differentiation defect by the Msi2 KD. The Msi2-KD C2C12 cells expressing Msi2 by infection of a retroviral Msi2 vector (shMsi2 + Msi2 OE, Fig. 3A-iv) exhibited as many elongated MHC-positive myotubes as those in the control cells (shLuc + vector control, Figs. 3A-i and 3B-i). In contrast, the cells with shMsi2 and an empty vector showed smaller myotubes with low MHC expression (shMsi2 + vector control, Figs. 3A-iii and 3B-iii). A few cells in the latter group were also positive for MHC, but were either much small in size or had only one nucleus, suggesting impaired mature myocyte formation. Msi2-KD C2C12 cells with the control vector exhibited the differentiation and fusion indices of 10% and 1.3, respectively, whereas those with Msi2 OE exhibited these indices of 21% and 2.1 (Fig. 3C). Collectively, these results clearly exclude the possibility of an off-target gene KD and demonstrate that Msi2 is required for the differentiation of C2C12 cells into mature myocytes as well as for their fusion during the terminal differentiation step of myotube formation.

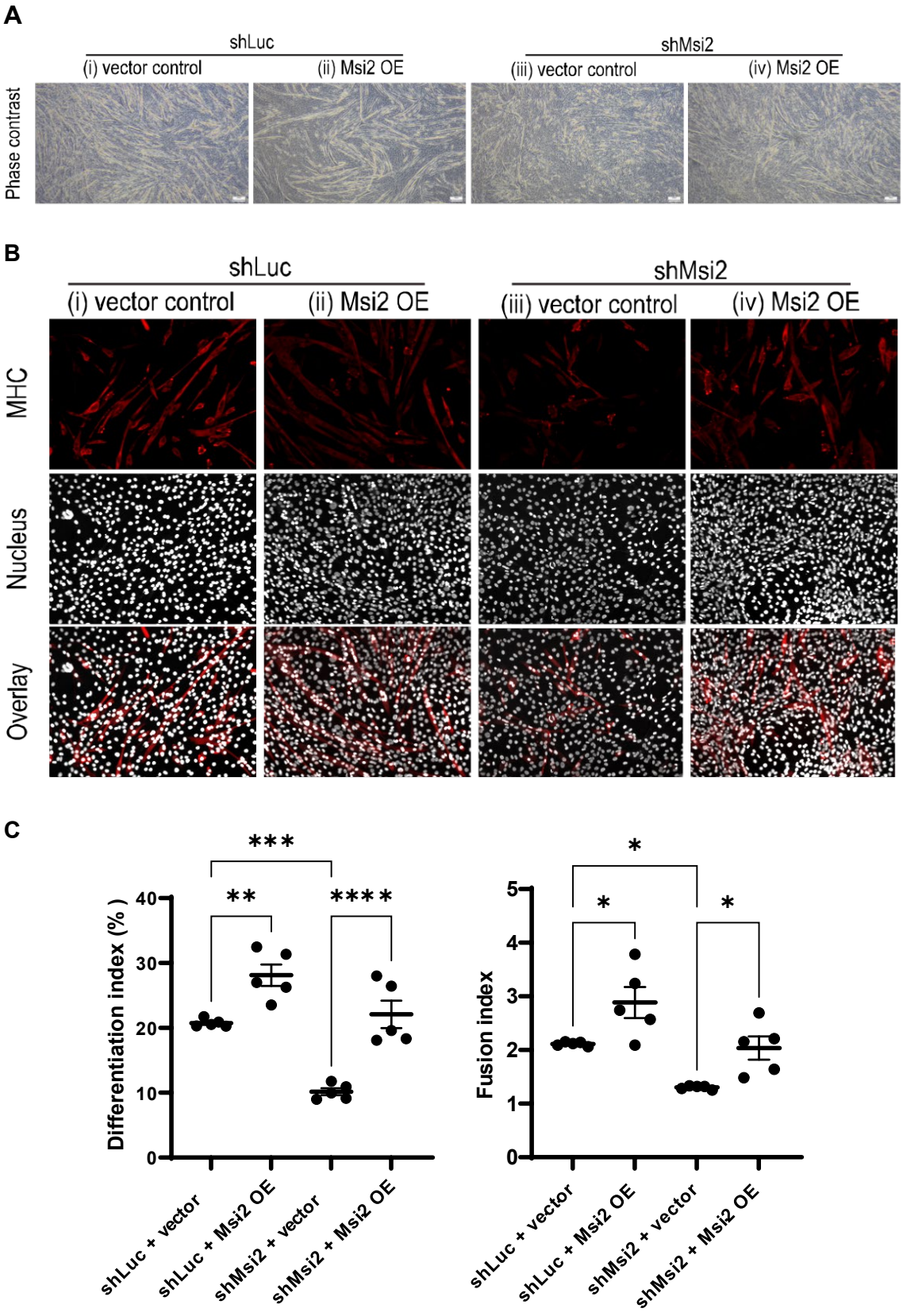
A
shLuc
shMsi2
(i) vector control
(ii) Msi2 OE
(iii) vector control
(iv) Msi2 OE
Phase contrast
B
shLuc
shMsi2
(i) vector control
(ii) Msi2 OE
(iii) vector control
(iv) Msi2 OE
MHC
Nucleus
Overlay
C
Differentiation index (%)
***
**
****
40
30
20
10
0
shLuc + vector
shLuc + Msi2 OE
shMsi2 + vector
shMsi2 + Msi2 OE
Fusion index
*
*
*
5
4
3
2
1
0
shLuc + vector
shLuc + Msi2 OE
shMsi2 + vector
shMsi2 + Msi2 OE

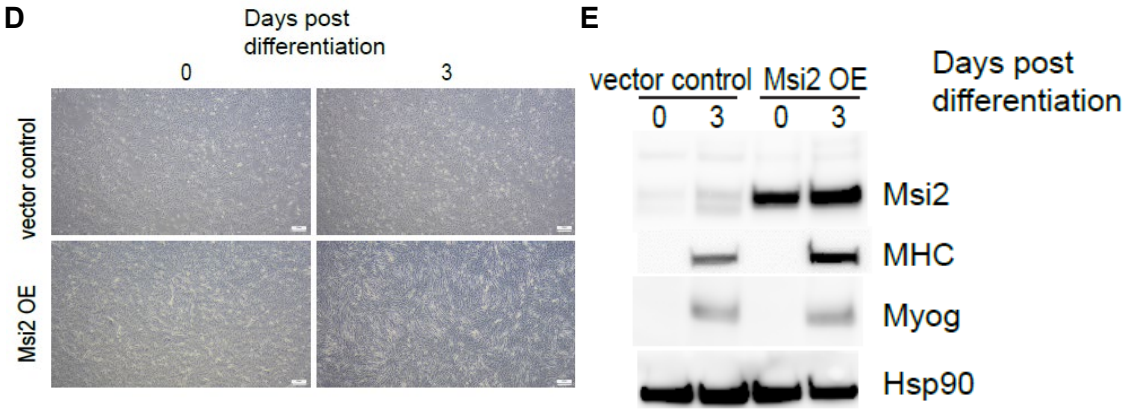

Fig. 3. Msi2 overexpression rescues Msi2 KD effect and promote C2C12 differentiation.

A. Phase-contrast images of shLuc or shMsi2 C2C12 cells rescued by vector control or Msi2 OE at day6 after differentiation induction.

B. Immunofluorescence staining of MHC in shLuc- or shMsi2-treated C2C12 cells infected with the control vector or the retroviral Msi2 vector (Msi2 OE).

C. Quantification of the differentiation index and fusion index. Each dot represents one field taken as shown in panel B. Five fields were picked in each experiment. One-way ANOVA with Tukey's multiple comparisons was used. *P<0.05, **P<0.01, ***P<0.001, ****P<0.0001.

D. Phase contrast microscope pictures of C2C12 cells infected with the control vector or the retroviral Msi2 vector (Msi2 OE) on day 0 (in GM) and day 3 after differentiation induction.

E. WB analysis of control C2C12 cells and those with Msi2 OE on day 0 (in GM) and day 3 after differentiation induction. Hsp90 was used as a loading control.

Enforced expression of Msi2 promotes myotube formation

During the experiments mentioned above to assess the on-target shRNA effects, I noticed that Msi2 overexpression alone could increase the formation of elongated myotubes (shLuc + Msi2 OE, Figs. 3A-ii and 3B-ii). In fact, differentiation and fusion indices were significantly higher in the cells expressing shLuc and Msi2 OE than in control cells with shLuc and vector control. I repeated the Msi2 overexpression experiment without co-introduction of any shRNA constructs and observed a similar enhancement of myocyte differentiation as early as 3 days after differentiation induction (Fig. 3D). Immunoblotting analysis showed that the MHC protein was further upregulated by Msi2 OE compared with the vector control (Fig. 3E, MHC), confirming the direct and functional impact of Msi2 in the promotion of differentiation. Interestingly, Msi2 OE did not lead to an increase in the Myog protein expression (Fig. 3E, Myog). This finding provided another evidence for a role of Msi2 independent of or downstream to Myog.

The RRM1 RNA binding ability and the C-terminal region of Msi2 are required for myocyte differentiation

Since Msi2 contains two functional domains for RNA binding, I next examined whether the RNA binding function is necessary for Msi2 to promote myocyte differentiation. To test this idea, I introduced the control vector, or a retroviral vector encoding wild-type (WT) Msi2 or one of the Msi2 mutants into C2C12 cells to observe their impacts on myoblast differentiation (Fig. 4A). The RNA binding domain mutant (RBD mutant) variant contains three point mutations in the RRM1 domain (Phe64, Phe66, and Phe69 to Leu), which lead to the loss of target binding function[32]. The Msi2 1-190 variant has only the first 190 amino acids (AA), including the RRM1 and RRM2 domains, but without the C-terminal part. The RRM1Δ and RRM2Δ variants lack the RRM1 domain (21-101 AA) or the RRM2 domain (110-187 AA), respectively. All the above Msi2 constructs are tagged with FLAG and HA at the N-terminus. WB analysis using an anti-FLAG antibody showed successful overexpression of all the Msi2 constructs in the C2C12 cells (Fig. 4B). Although the RBD mutant and RRM2Δ Msi2 had much lower expression levels than the others, most of the cells in all samples were GFP positive, suggesting successful retroviral transduction (Fig. 4C, GFP). On day3 after differentiation induction, WT and RRM2Δ Msi2 OE C2C12 cells exhibited more MHC-positive compared to the vector control cells, indicating promoted differentiation (Fig. 4C). The 1-190 and RRM1Δ OE cells showed comparable numbers of MHC-positive cells compared with the control cells, and interestingly, the RBD mutant OE even showed a trend of less differentiation than the vector control. Differentiation indices are also significantly increased in the WT and RRM2Δ Msi2 OE cells but not in the others compared to the vector control (Fig. 4D). There was no significant difference in fusion indices among all the groups since myocyte fusion mainly happens in the late differentiation stage (Fig. 4E). These MHC IF staining results correlated with the MHC

WB analysis result, which also showed higher MHC expression levels in WT and RRM2Δ than the others (Fig. 4B, MHC). These data demonstrated that RRM2Δ Msi2, but not the other variants, has a similar differentiation-promoting function as WT Msi2, indicating that the RRM1 RNA binding ability and the C-terminal region of Msi2 are required for Msi2 to regulate myoblast differentiation and that the RRM2 domain is not necessary for the Msi2 function.

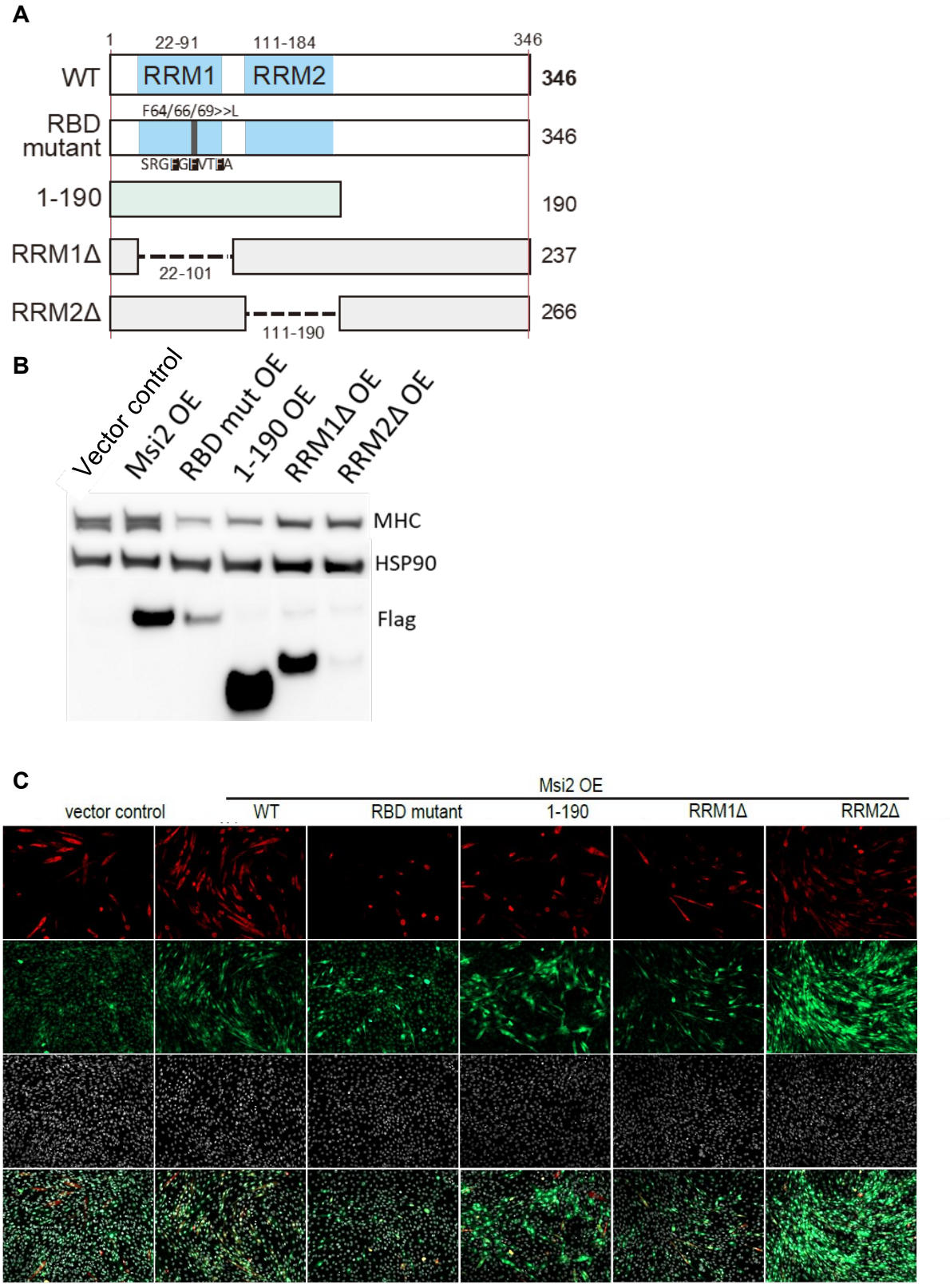
A
1
22-91
111-184
346
WT
RRM1
RRM2
346
RBD mutant
F64/66/69>>L
346
1-190
190
RRM1Δ
22-101
237
RRM2Δ
111-190
266
B
Vector control
Msi2 OE
RBD mut OE
1-190 OE
RRM1Δ OE
RRM2Δ OE
MHC
HSP90
Flag
C
Msi2 OE
vector control
WT
RBD mutant
1-190
RRM1Δ
RRM2Δ
MHC
GFP
Nucleus
Overlay

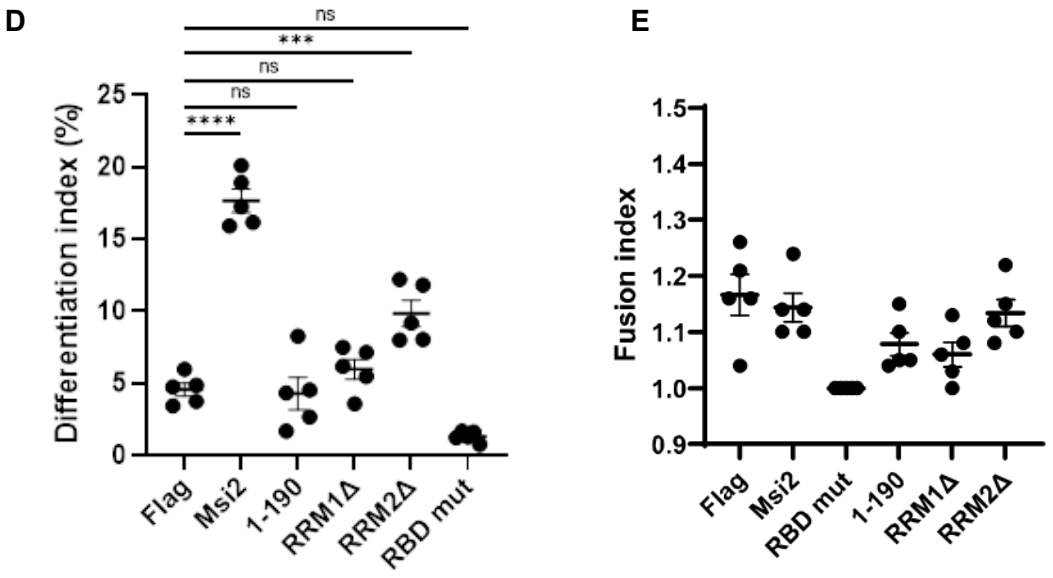

Fig. 4. The RRM1 and c-terminus but not RRM2 of Msi2 are required for promoting myocyte differentiation

A. Schematic figure showing the structure of WT mMsi2 and its mutants.

B. WB analysis of C2C12 cells treated with the control vector, or those overexpressing WT Msi2 or its mutant at day 3 of differentiation. FLAG tag level represents the OE level of Msi2. Hsp90 was used as a loading control.

C. Immunofluorescence staining of MHC in C2C12 cells treated with the vector control or those overexpressing WT or mutant Msi2 on day 3 of differentiation.

D, E. Quantification of the differentiation index **(D)** and fusion index **(E)**. Each dot represents one field taken as shown in panel C with 5 fields taken in total. One-way ANOVA with Tukey's multiple comparisons was performed. *P<0.05, **P<0.01, ****P<0.0001.

Msi2 KD affects mitochondrial membrane potential without affecting their biogenesis and function

Since previous data suggested that Msi2 regulates myoblast differentiation independent of MRFs, I then focused on other factors that are necessary for myogenesis to understand the molecular mechanism underlying the Msi2-dependent differentiation. First, I hypothesized that Msi2 may regulate mitochondrial biogenesis, function, and mitophagy, which are critical for myoblast differentiation[9,42]. Since the mitochondria amount and function are known to be increased dramatically during myoblast differentiation[43], I analyzed the effect of Msi2 KD on the amount and respiration function of mitochondria in myoblast stage C2C12 cells to see if Msi2 directly regulates mitochondria independent of its impact on the myogenic program. To assess mitochondrial biogenesis, I analyzed the mitochondrial DNA (mtDNA) content in the cells, a commonly used method for mitochondria quantification[44,45]. The mtDNA level is comparable between the control and Msi2-KD cells (Fig. 5A), suggesting Msi2 is not implicated in mitochondrial biogenesis. Next, I assessed the mitochondrial respiratory function using the Seahorse assay (Fig. 5B). The control and Msi2-KD cells exhibited a similar pattern of oxygen consumption rate (OCR) change during the assay. Basal and maximal respiration, measured before oligomycin injection and after cyanide-*p*-trifluoromethoxyphenylhydrazone (FCCP) injection, were comparable between the control and Msi2-KD groups (Fig. 5C), suggesting Msi2 does not regulate mitochondrial respiration function in myoblasts. In addition to the mitochondrial respiratory function, I analyzed mitochondrial membrane potential ($\Delta\Psi m$) by Mitotracker Deep Red staining, which is a $\Delta\Psi m$-dependent dye. Flow cytometry analysis of cells stained with Mitotracker Deep Red showed that the Msi2-KD cells have 17% lower Mitotracker Deep Red staining than the control cells (Fig. 5D). Since the mtDNA results indicate that mitochondrial biogenesis was not affected by Msi2 KD (Fig. 5A), the lower Mitotracker Deep Red

staining implies lower ΔΨm but not mitochondria content in the Msi2-KD cells. Rather than the mitochondrial respiratory function, which is shown to be unaffected by Msi2 knockdown (Fig. 5C), the low ΔΨm can be associated with triggering autophagy or mitophagy[46,47]. Therefore, I then examined if Msi2 KD affects autophagy during myoblast differentiation.

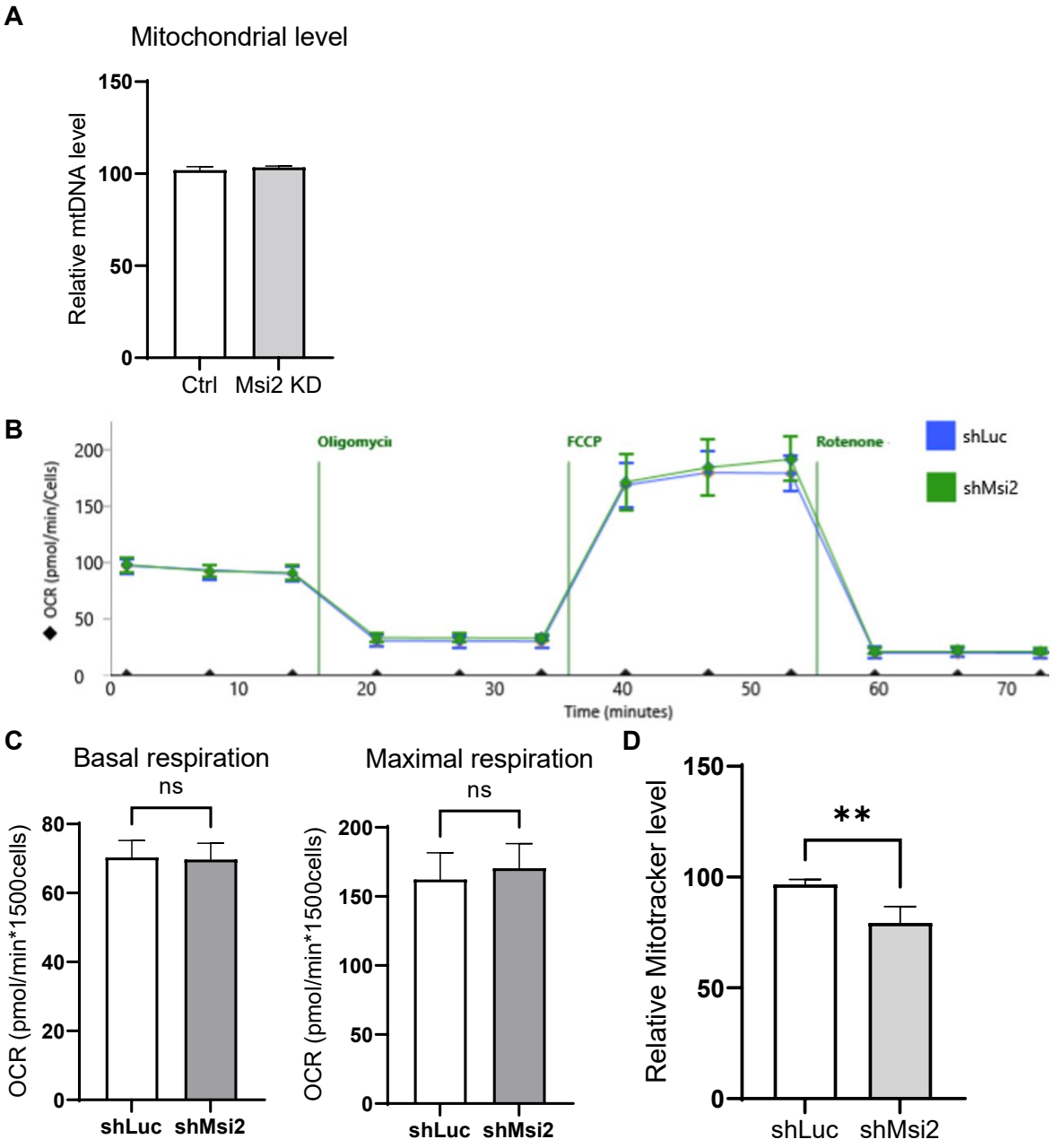
A
Mitochondrial level
Relative mtDNA level
150
100
50
0
Ctrl
Msi2 KD
B
Oligomycin
FCCP
Rotenone
shLuc
shMsi2
OCR (pmol/min/Cells)
200
150
100
50
0
0
10
20
30
40
50
60
70
Time (minutes)
C
Basal respiration
ns
OCR (pmol/min*1500cells)
80
60
40
20
0
shLuc
shMsi2
Maximal respiration
ns
OCR (pmol/min*1500cells)
200
150
100
50
0
shLuc
shMsi2
D
Relative Mitotracker level
**
150
100
50
0
shLuc
shMsi2

Fig. 5. Msi2 KD affects mitochondrial membrane potential without affecting their biogenesis and function

A. qPCR analysis of the mtDNA content in shLuc- or shMsi2-treated C2C12 cells in growth media.

B. Seahorse analysis of mitochondrial respiratory function of undifferentiated shLuc- and shMsi2-treated C2C12 cells (n=6).

C. Basal and maximal respiration of undifferentiated shLuc- or shMsi2-treated C2C12 cells during the Seahorse analysis as shown in panel B. Unpaired *t*-test was used. Ns: no significance.

D. Flow cytometry analysis of Mitotracker Deep Red staining intensity in undifferentiated shLuc- or shMsi2-treated C2C12 cells (n=4). Unpaired *t*-test was used. **P<0.01.

Msi2 regulates myoblast differentiation through autophagy

The data presented so far have shown that Msi2 is not only essential but also sufficient for myoblast differentiation, independent of the expression of MRFs. Previous studies showed that autophagy and mitophagy processes are required for myoblast differentiation[9,48]. To test whether Msi2 regulates myoblast differentiation through autophagy, I first analyzed the participation of autophagy by analyzing free LC3A and autophagosomal LC3A (LC3A-I and LC3A-II, respectively) in cell lysates by WB. As LC3-II is associated with autophagosomal membranes via lipid modification, it is an indicator of autophagy[49–51]. I observed an increase of the LC3A-I and LC3A-II levels in the control cells during the differentiation but not obviously in Msi2-KD cells (Fig. 6A), suggesting the possibility that Msi2 participates in autophagy by regulating the LC3 level. Interestingly, the mRNA level of LC3A was comparable between shLuc and shMsi2 cells (Fig. 6B), suggesting that Msi2 may regulate LC3A translation. I further analyzed the number of LC3A puncta in the cytoplasm by immunofluorescence staining, which is another indicator of autophagy[52]. Msi2-KD cells had less overall LC3A staining in the cell and significantly less cytoplasmic LC3A puncta per cell (Fig. 6C, D), indicating less autophagosome formation in the Msi2-KD cells.

To confirm that the autophagy defect in Msi2-KD cells is the cause for the inhibition of differentiation, I tested if activation of autophagy could rescue the Msi2-KD phenotype. To induce autophagy, I used a small peptide Tat-Beclin1-D11, which is known as an autophagy inducer by binding to autophagy repressor GAPR1 to release Beclin1[53]. A scrambled peptide Tat-Beclin1-L11S was used as the negative control. By the Tat-Beclin1-D11 peptide treatment, both control and Msi2-KD cells formed more and thicker myotubes on day 5 after differentiation induction (Fig. 6E and F). The differentiation index of Msi2-KD cells with the scrambled control peptide was significantly increased from 13% to 29%, which was comparable to 34% in control cells, suggesting the differentiation

defect in Msi2-KD cells was fully rescued by autophagy induction (Fig. 6G). The Tat-Beclin1-D11 treatment significantly increased the fusion index of Msi2-KD cells from 1.3 to 2.6 as well, although the rescue was partial compared to 4.1 in the control cells (Fig. 6H). Surprisingly, Tat-Beclin1-D11 significantly increases both differentiation and fusion index even in the control cells (Fig. 6G and H), implying promotion of differentiation by autophagy activation. WB analysis confirmed that the LC3A-II level was increased in both control and Msi2-KD cells by the Tat-Beclin1-D11 treatment, confirming autophagy activation by the Tat-Beclin1-D11 treatment (Fig. 6I). Taken together, the Tat-Beclin1-D11 peptide successfully rescued the autophagy level and the differentiation defect in Msi2-KD cells, suggesting that Msi2 regulates myoblast differentiation via autophagy.

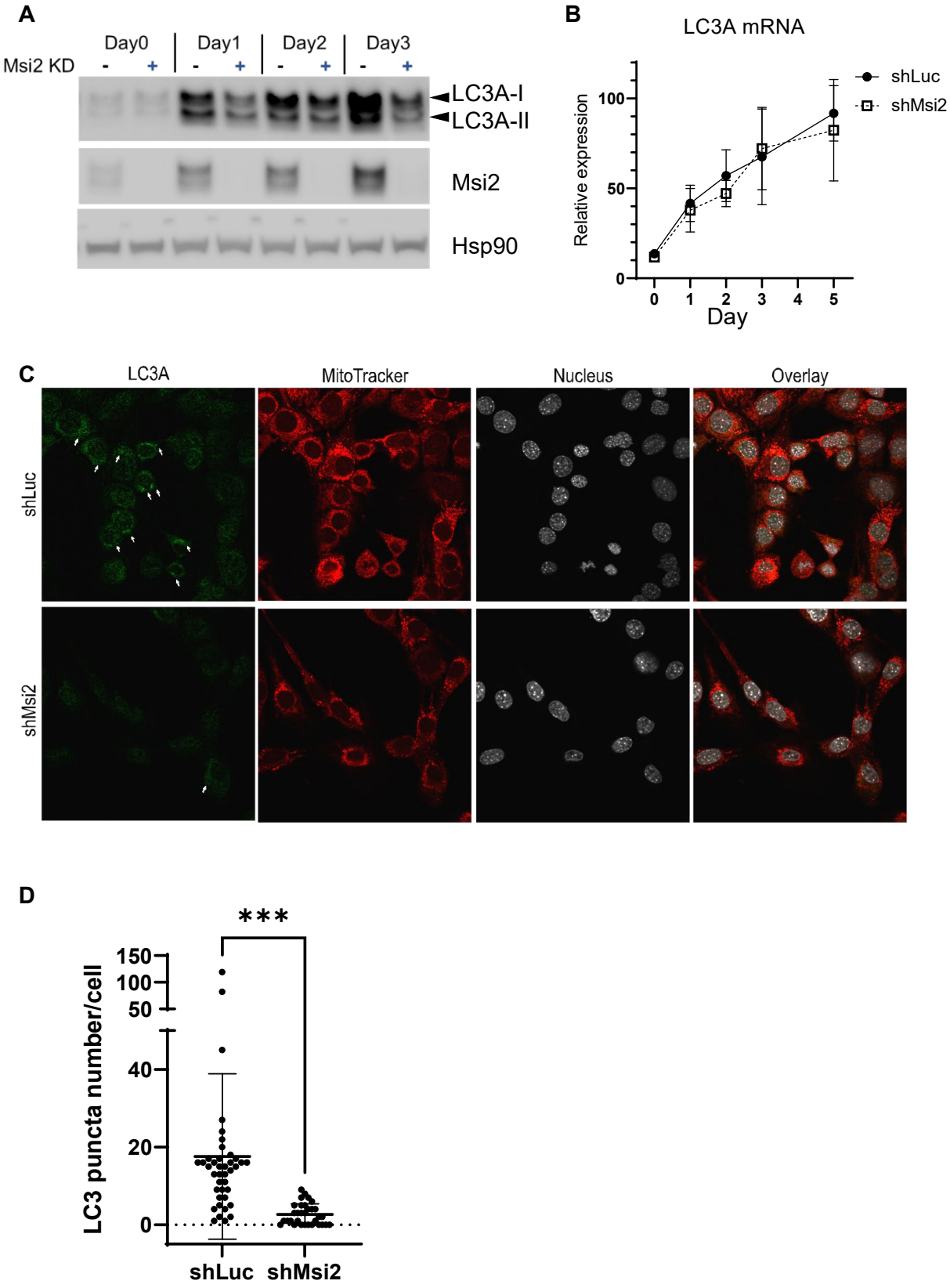
A
Day0
Day1
Day2
Day3
Msi2 KD
- + - + - + - +
LC3A-I
LC3A-II
Msi2
Hsp90
B
LC3A mRNA
Relative expression
100
50
0
0 1 2 3 4 5
Day
shLuc
shMsi2
C
LC3A
MitoTracker
Nucleus
Overlay
shLuc
shMsi2
D
***
LC3 puncta number/cell
150
100
50
40
20
0
shLuc
shMsi2

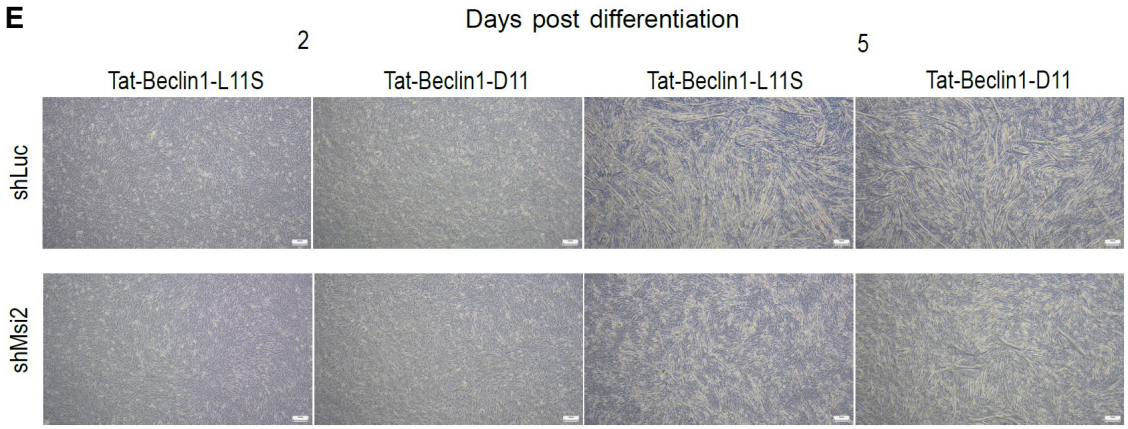
E
Days post differentiation
2
5
Tat-Beclin1-L11S
Tat-Beclin1-D11
Tat-Beclin1-L11S
Tat-Beclin1-D11
shLuc
shMsi2

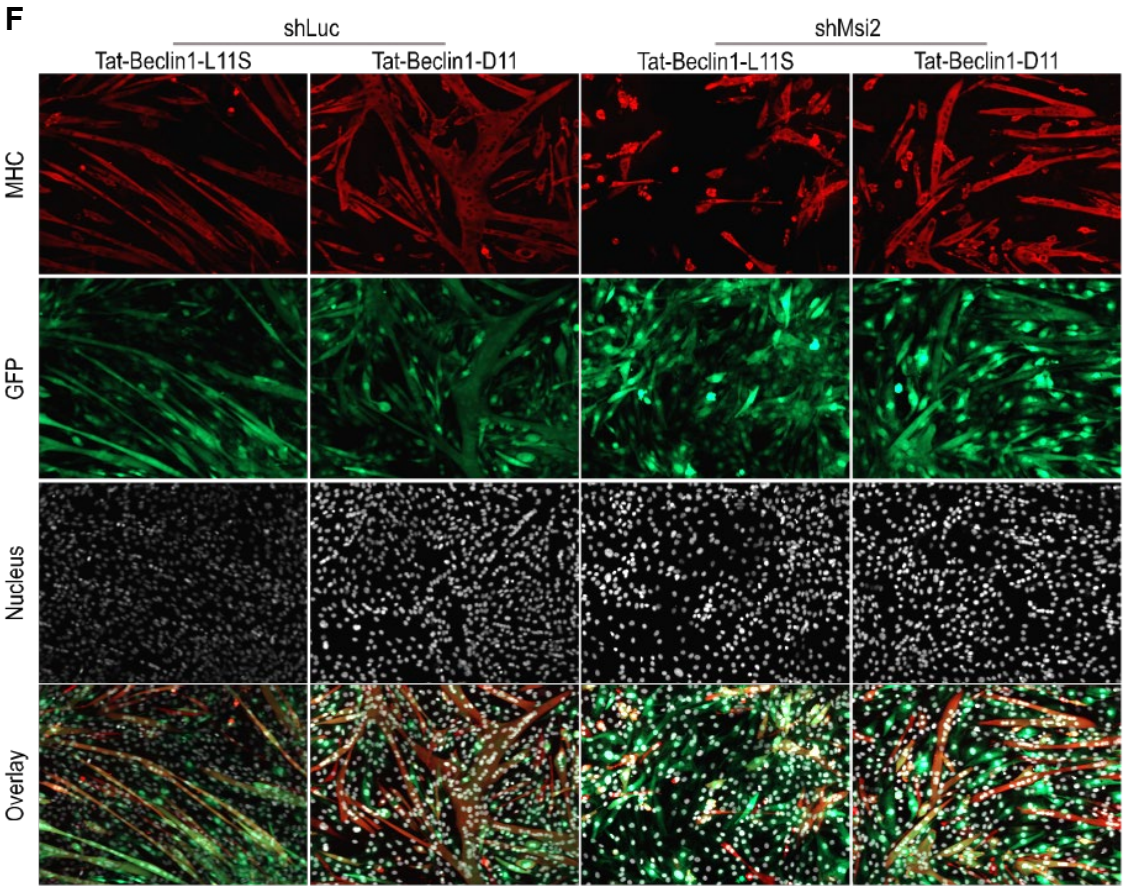
F
shLuc
shMsi2
Tat-Beclin1-L11S
Tat-Beclin1-D11
Tat-Beclin1-L11S
Tat-Beclin1-D11
MHC
GFP
Nucleus
Overlay

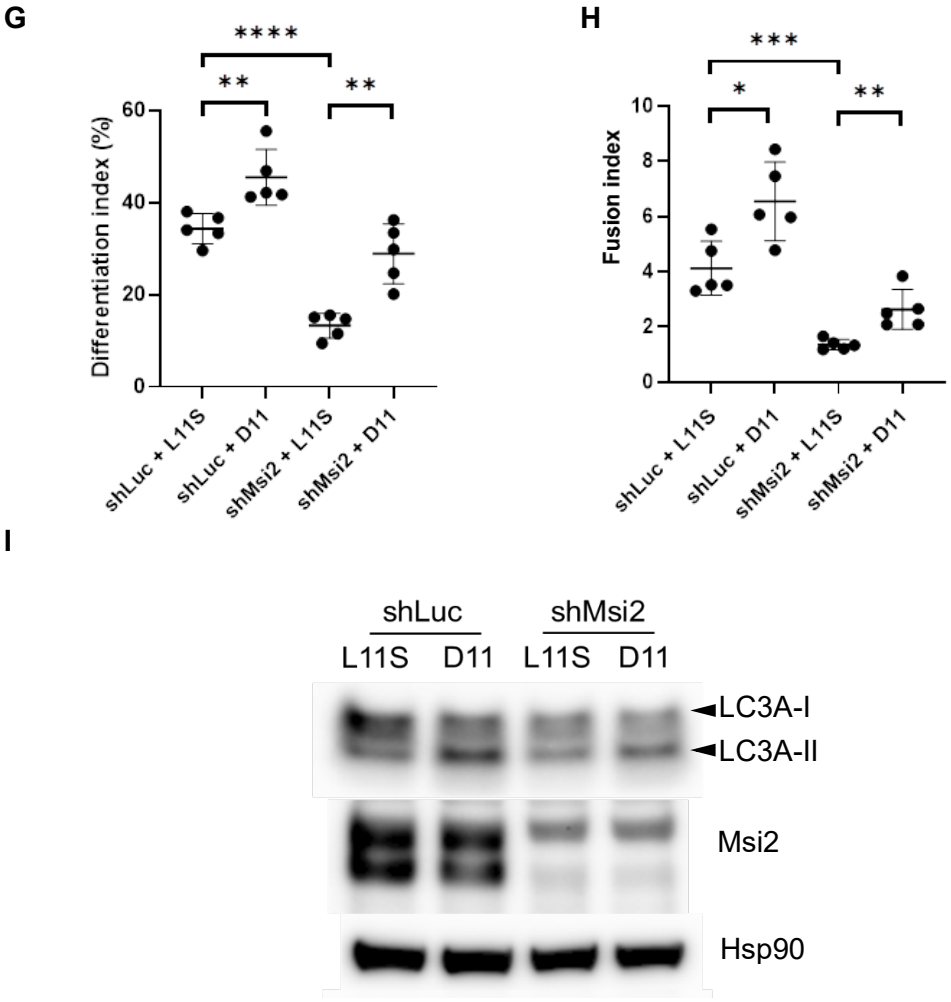

Fig. 6. Msi2 regulates autophagy during C2C12 differentiation

A. WB analysis of the LC3A-I (top band) and LC3A-II (bottom band) levels in control (-) and Msi2-KD (+) C2C12 cells during differentiation.

B. Changes in the LC3A mRNA level in shLuc- and shMsi2-treated C2C12 cells during differentiation. Data from 3 independent experiments were included.

C. Immunofluorescence staining of LC3A in shLuc- and shMsi2-treated C2C12 cells on day1 of differentiation. White arrows indicate LC3A puncta in the cytoplasmic area.

D. Quantification of the cytoplasmic LC3A punctate number in the cell. Forty shLuc-treated cells and 32 shMsi2-treated cells from 3 different fields in each group were

analyzed. Each dot represents the number of puncta in one cell. Unpaired *t*-test, ***P<0.0001.

E. Phase contrast images of shLuc- or shMsi2-treated C2C12 cells with 100 μM Tat-Beclin1-L11S scramble negative control or Tat-Beclin1-D11 peptide treatment on day2 and day5 after differentiation induction.

F. Immunofluorescence staining of MHC in shLuc- or shMsi2-treated C2C12 cells with 100 μM Tat-Beclin1-L11S control or Tat-Beclin1-D11 peptide treatment on day5 after differentiation induction

G, H. Quantification of the differentiation index **(G)** and fusion index **(H)**. Each dot represents one field taken as shown in panel F. Five fields were picked in each experimental group. One-way ANOVA analysis with Tukey's multiple comparisons was used, *P<0.05, **P<0.01, ***P<0.001, ****P<0.0001.

I. WB analysis of LC3A-I (top band) and LC3A-II (bottom band) in control and Msi2-KD C2C12 cells treated with scrambled negative control (L11S) or Tat-Beclin1-D11 (D11) on day2 after differentiation induction

Msi2 gene trap mutant mice exhibit defective skeletal muscle

To validate the role of Msi2 in skeletal muscle, I used a functional *Msi2*-knockout (KO) mouse model that is achieved by the insertion of a gene trap vector in between the exon 5 and 6 of the *Msi2* gene, resulting in early transcription termination and eventually degradation of Msi2 protein (Fig. 7A and B). The Msi2 gene trap (Gt) mice exhibited 27% less body mass compared to their wild type (WT) litter mates (Fig. 7C). The masses of extensor digitorum longus (EDL) muscles and soleus muscle of Gt mice were also 27% and 38% lower than the WT control, respectively (Fig. 7D). And the soleus muscle of Gt mice exhibited a pale color compared to WT, suggesting the lower myoglobin level (Fig. 7E). These data suggest abnormal skeletal muscle development in the *Msi2* Gt mice. To examine if Msi2 loss affects the muscular function, I performed treadmill exhaustion test and compared the total running distance between WT and *Msi2* Gt. The *Msi2* Gt female mice could only run for 34 meters before exhaustion on average, compared to 182 meters of the control female mice, indicating significantly less endurance training abilities of the *Msi2* Gt mice (Fig. 7F). A similar pattern was observed in male mice I, suggesting no significant contribution from sexual difference on the Msi2 KO phenotype. In the open field test, *Msi2* Gt mice moved significantly less than WT littermates (Fig. 7G). However, the stereotypic behavior times were comparable between *Msi2* Gt mice and WT littermates, suggesting that lower locomotor activity and lower endurance training ability were likely due to physical but not neurological defects in the *Msi2* Gt mice (Fig7. H). In summary, *Msi2* Gt mice exhibited smaller and less functional skeletal muscles, confirming that Msi2 is critical for skeletal muscle development and function in vivo.

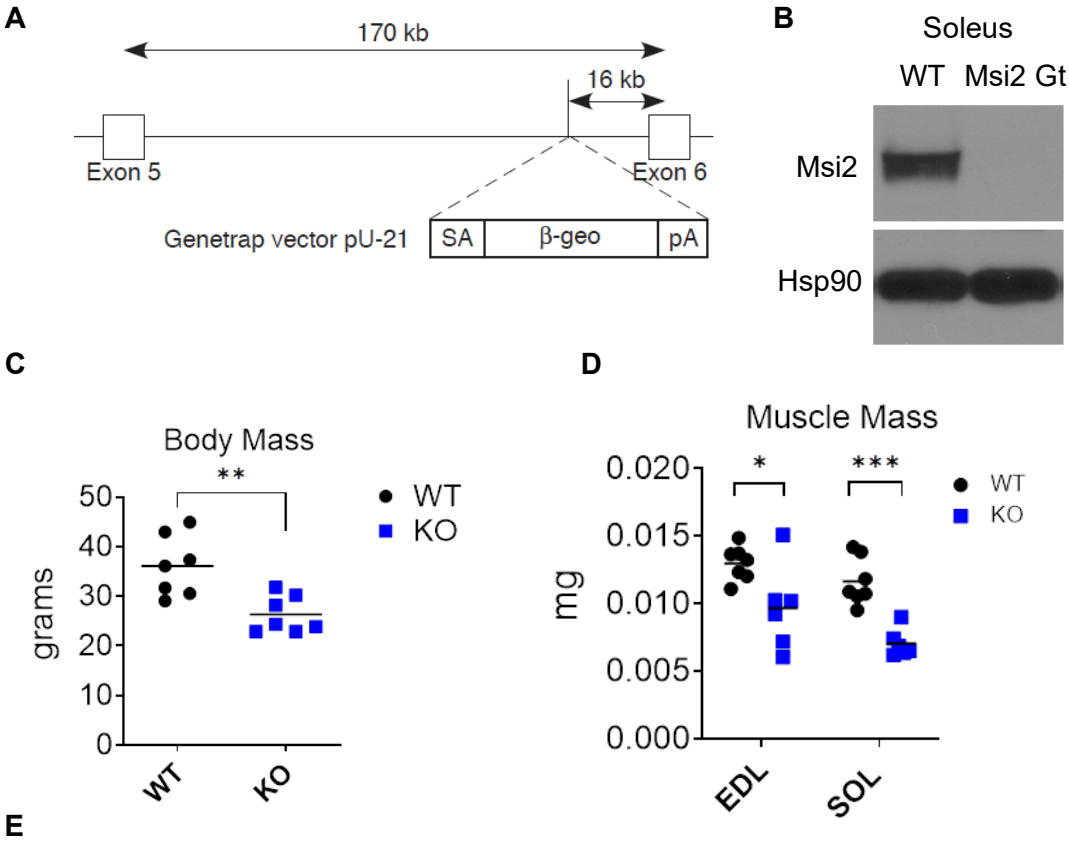
A
170 kb
16 kb
Exon 5
Exon 6
Genetrap vector pU-21
SA
β-geo
pA
B
Soleus
WT
Msi2 Gt
Msi2
Hsp90
C
Body Mass
**
grams
50
40
30
20
10
0
WT
KO
WT
KO
D
Muscle Mass
*
***
mg
0.020
0.015
0.010
0.005
0.000
EDL
SOL
WT
KO
E
WT Soleus
KO Soleus

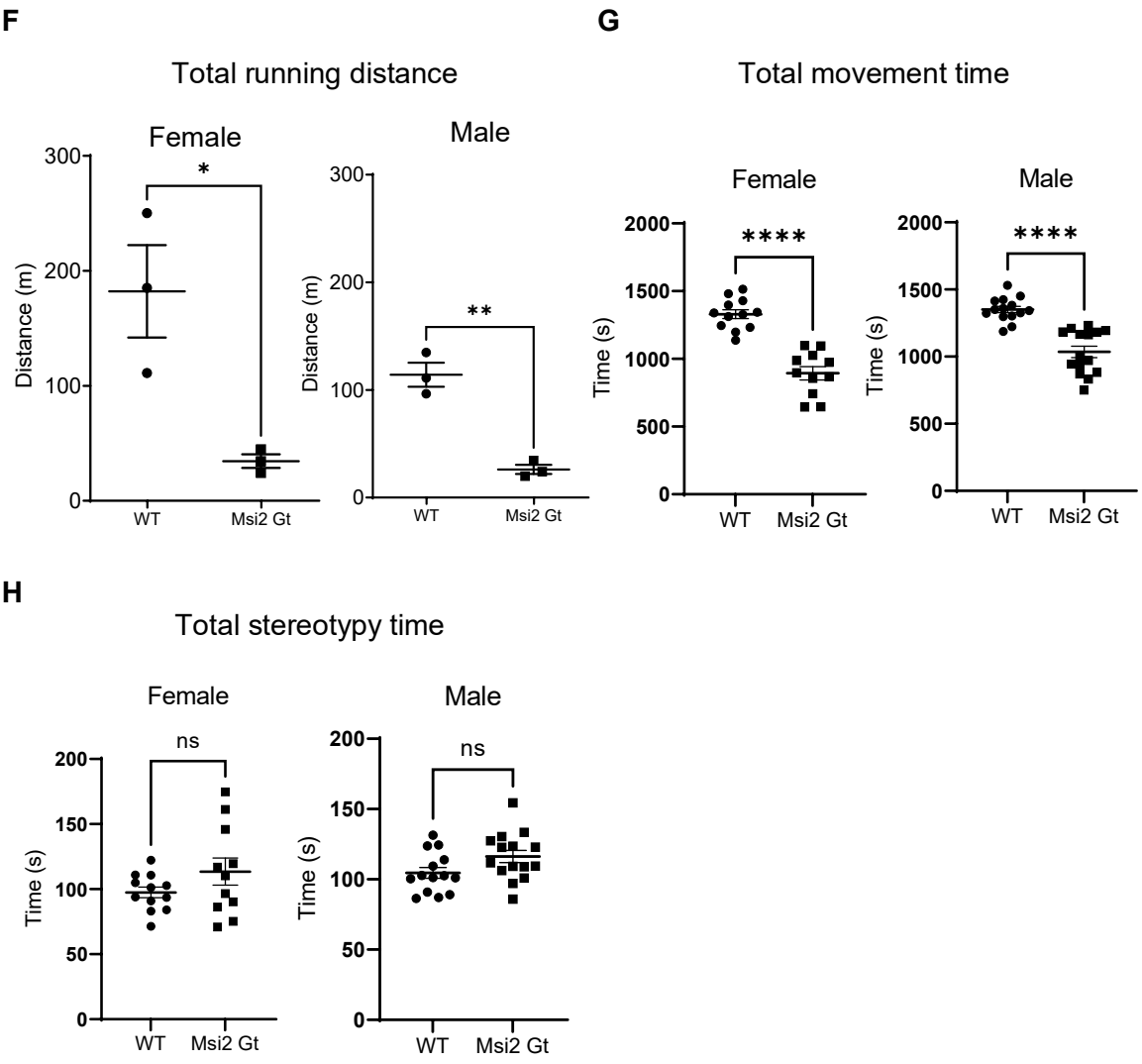

Fig. 7. *Msi2* gene trap KO (Gt) mice exhibit defective skeletal muscles

A. Schematic figure of Msi2 mutant allele generated by an insertion of the gene trap vector pU-21. The splice acceptor sequence (SA) and polyadenylation signal (pA) on the gene trap vector will result in early termination of transcription.

B. WB analysis of the Msi2 level in soleus muscle of WT control or *Msi2* Gt mice. Hsp90 was used as a loading control.

C. Body mass, and **D.** EDL and soleus muscles mass of WT or Msi2 Gt mice (n = 7)

E. Representative images of WT or *Msi2* Gt soleus muscles.

F. Total running distance of WT or *Msi2* Gt mice in treadmill exercise assay (n = 3).

G. Movement time of male and female WT or *Msi2* Gt mice in the open field test.

H. Stereotypy time of male and female WT or *Msi2* Gt mice in the open field test. *P<0.05, **P<0.01, ****P<0.0001. Each dot represents an individual animal. Error bars represent ± SEM.

Discussion

The regulation of myogenesis has been extensively studied for decades. Although the MRF family of transcription factors are known to be the master regulators of myogenesis[5,54], recent studies unveiled many new aspects of the regulation of myogenesis, including post-transcriptional regulation, autophagy, mitochondria, metabolism, and so on[8,9,16,42,55,56] . Msi2, a cell fate regulator of neural, hematopoietic, and leukemic stem cells, is known to be expressed in skeletal muscle tissue, but little has been reported about its function in skeletal muscle tissue[57,58]. Therefore, I tended to investigate if Msi2 directs cell fate decisions in myogenesis like its functions in other systems.

C2C12 myoblast is widely used as a model for studying the myogenesis process[37]. Msi2 KD in C2C12 cells severely impaired the differentiation and fusion of the cells (Fig. 2), indicating that Msi2 is essential for the myoblast differentiation process. Moreover, Msi2 OE is not only able to rescue the Msi2 KD phenotype but also increases the differentiation and fusion indices in control cells (Fig. 3C), indicating the role of Msi2 in promoting myoblast differentiation. Interestingly, either Msi2 KD or OE caused no effect on the expression of Myogenin (Fig. 2A and Fig. 3E), suggesting that the Msi2 function is independent or downstream of the canonical myogenic program regulator MRFs. Studies that identified new genes involved in myogenesis usually demonstrated the regulation of MRFs by the new genes, such as RBPs HuR, KSRP, and Lin-28[16]. It is rare to see a gene behaves like Msi2 that its loss severely blocks myoblast differentiation while maintaining intact myoblast proliferation and expression of MRFs, implying Msi2 is downstream of independent of MRFs. With these findings, I identified Msi2 as a novel regulator of myoblast differentiation.

The downstream mechanism of Myog is not fully understood. As an RBP, Msi2 may regulate myogenic gene expression post-transcriptionally. The RNA binding function of Msi2 is required for myoblast differentiation, supported by the evidence that RNA binding ability deficiency abolished the ability of Msi2 to promote differentiation (Fig. 4D). Interestingly, the C-terminal region of Msi2 is also required for its function, although the role of the C-terminal region is not well studied yet. Unlike Msi1, Msi2 does not have a protein binding domain to interact with poly (A)-binding protein[24]. Instead, a site-specific phosphorylation in the C-terminal region is reported to convert the canonical translational repressor function of Msi2 to translational activation[59]. This evidence could explain why the loss of the C-terminus region nullifies the function of Msi2 in myoblast differentiation.

The previous Msi2-KD experiments have shown that Msi2 functions independently of MRFs. To understand the molecular mechanism, I focused on other pathways that are not strongly controlled by MRFs during myoblast differentiation. I first hypothesized that Msi2 may regulate mitochondria. Because mitochondrial biogenesis and function are known to be upregulated during myoblast differentiation[43], I decided to assess mitochondrial biogenesis and function in the myoblast stage without differentiation induction to exclude the effect from the MRFs. Although the mtDNA content and mitochondrial respiratory function appeared to be unaffected by the Msi2 KD, Mitotracker Deep Red staining was significantly decreased in Msi2-KD myoblasts, suggesting reduced mitochondrial membrane potential ($\Delta\Psi m$). This result may seem contradictory since $\Delta\Psi m$ is usually correlated with respiratory function. However, $\Delta\Psi m$ also has other biological functions besides generating ATP, such as triggering mitophagy[46]. Intrigued by this data, I investigated if Msi2 regulates autophagy during myoblast differentiation.

Autophagosome formation is one of the key steps for autophagy activation. The conversion of a cytosolic form of LC3 (LC3-I) to a phosphatidylethanolamine-conjugated autophagosomal membrane-bounded form (LC3-II) is essential for the initiation of autophagosome formation. Therefore, LC3-II is widely recognized as an autophagosomal marker[52,60]. By Msi2 KD, both LC3A-I and LC3A-II were substantially decreased without an obvious change in the LC3A-II/LC3A-I ratio (Fig. 6A). This result indicates that Msi2 regulates the protein level rather than activation of LC3A. This hypothesis is further supported by the evidence that Msi2 KD did not regulate LC3A mRNA level (Fig. 6B). This data suggests that Msi2 may not regulate the LC3A protein level indirectly through other transcriptional regulators, for example FoxO3[61], but directly regulates its mRNA translation. To further confirm whether Msi2 KD reduces autophagy activity and thereby impairs differentiation or Msi2 KD blocks differentiation and causes the reduction in the autophagy level, I tested if autophagy induction could rescue the differentiation defect caused by the Msi2 KD. Autophagy induction is commonly induced by starvation or inhibition of the mTOR signaling. However, starvation and mTOR inhibition are reported to impair C2C12 myoblast differentiation, likely due to the requirement of mTOR activation in myoblast differentiation rather than autophagy activation [8,62,63]. To induce autophagy without affecting the mTOR signaling, I used a small peptide, Tat-Beclin1-D11, which is known to induce autophagy by competitively binding to autophagy repressor GAPR1 to release Beclin1[53]. The Tat-Beclin1-D11 peptide treatment increased the LC3A-II level in both control and Msi2-KD cells and successfully rescued the differentiation defect in Msi2-KD cells (Fig. 6E-I), suggesting that the autophagy inhibition in Msi2-KD cells is the cause for the differentiation defect. Collectively, these data demonstrate the molecular mechanism that Msi2 regulates myoblast differentiation via autophagy.

Other than in vitro, Msi2 is also vital for skeletal muscle development and function in vivo. The Msi2 Gt mice exhibited lower body mass and muscle mass than the wild-type (WT) littermates (Fig. 7C and D). The pale color in *Msi2* Gt soleus muscle suggests low myoglobin levels or potential muscle fiber-type switching since slow-twitch muscle (e.g. soleus) is known to be high in myoglobin and red in color[64]. Results of both open field test and treadmill exhaustion test showed that *Msi2* Gt mice have lower moving ability, suggesting defective muscular function. Above all, these data provided evidence for the importance of Msi2 in skeletal muscle health in vivo.

The limitations of this study should also be mentioned. Since the *Msi2* Gt mouse is a germline mutation model, Msi2 loss in other systems rather than skeletal muscle may inevitably contribute to the phenotype. For example, Msi2 is highly expressed in neural stem cells and progenitors. Although Msi1 and Msi2 play compensatory roles in the development of the central nervous system[25], and the open field test result implies no obvious neurological defects in *Msi2* Gt mice (Fig. 6H), the possibility that loss of Msi2 in the nervous system affects skeletal muscle performance cannot be completely excluded. To eliminate this possibility, future study will be performed on skeletal muscle-specific conditional *Msi2*-KO mice.

In summary, the results of this study revealed that Msi2 is a novel regulator of myogenesis via activation of autophagy, which is a key step in the myogenic differentiation of myoblasts. Since this is the first study for a role of Msi2 in the regulation of autophagy in myogenesis, these findings should lead to a better understanding of the autophagy-related functions of Msi2 in determining cell fate in neural, hematopoietic, and leukemic stem cells. Since autophagy activation by the Tat-Beclin1-D11 peptide was shown to promote myoblast differentiation, this finding may provide a potential therapeutic strategy for myopathies accompanying abnormal autophagy levels.

Acknowledgement

First, I would like to express my sincere thanks to my advisor Dr. Takahiro Ito for his guidance and support on this project.

Besides my advisor, I would like to thank all the lab members that provided their help on this project: Dr. Ayuna Hattori, Dr. Kenkyo Matsuura, Rio Watson, Futaba Kato, Kristen Mackeil, and Simran Rajput.

I also would like to thank all our collaborators for their precious help on this project:
Dr. Aaron Beedle, Binghamton University
Dr. Hang Yin, Dr Amelia Yin, Dr. Jarrod A. Call, Dr. Anna Nichenko, Albi Schifino, University of Georgia
Dr. Takeshi Noda, Yugo Tsunoda, Kyoto University
Dr. Takaho Tsuchiya, University of Tsukuba

I would like to offer my special thanks to the scholarship support from the Division of Graduate Studies, Kyoto University.

Last but not least, I would like to thank my family: my parents and especially my wife for supporting me spiritually throughout my graduate student life.

Methods and materials

Mice

The Msi2 mutant mice, B6; CB-*Msi2*$^{Gt(pU-21T)2Imeg}$, was made and established by gene trap mutagenesis as described previously[31]. Mice were bred and maintained in the facility of the University Research Animal Resources at University of Georgia, Athens. All mice were 4–9 months old, age matched and randomly chosen for experimental use. No statistical methods were used for sample size estimates. All animal experiments were performed according to protocols approved by the University of Georgia Institutional Animal Care and Use Committee.

Mouse treadmill exhaustion assay

Mice were trained for two days before the actual test. Treadmill was placed with 15˚ downhill for exhaustion test. On the training day, mice were placed on treadmill at 0 m/min for 25 min and 3 m/min for 5 min. On test day, mice were placed on treadmill for warming up at 3 m/min for 5 min. Then increase speed to 10 m/min, start counting time and observe for exhaustion for each individual mouse. Exhaustion was defined as staying on the shock pad for over 10 seconds. And shocks will be turned off after exhaustion. Increase speed by 5 m/min every 5 min until 25 m/min. Let mice run at 25 m/min no more than 15 min. The time of how long mice can run were recorded as soon as mice exhausted.

Open field test

Mouse open field activity monitors (16 inch × 16 inch SuperFlex Open Field, Omnitech Electronics) were used for the experiments. The following parameters were recorded for

the 30 min test session: total travel distance, movement time, horizontal activity count (horizontal beam breaks), total rest time (inactivity greater or equal to 1 second), stereotypy time, stereotypy episode count (stereotypy behavior greater or equal to 1 second was counted as 1 episode), vertical activity count (vertical beam breaks), and vertical activity time.

Cell culture, proliferation viral infection, and differentiation assays

The mouse C2C12 mouse myoblast cell line was maintained in Growth Media (GM; Dulbecco's Modified Eagle Medium (DMEM) with high glucose, 15% FBS (VWR), 1% non-essential amino acids (NEAA), 100 IU/ml penicillin, and 100 µg/ml streptomycin). For cell proliferation assays, the cells were plated in 96-well plates at the density of 1×10^4 cells/ml in GM. Cells were trypsinized and counted at indicated time points. Media was changed every 3 days. To infect cells with lentivirus or retrovirus, cells were plated in 60mm dish at 2×10^4 cells/ml, 3 ml/dish in GM. After 24 hours, viruses and 1ug/ml polybrene were added to the culture. After another 48 hours, cells were collected and replated for the following experiments. To induce differentiation of C2C12 myoblasts into myotubes, the cells were plated in 6-well plates at 4×10^4 cells/ml, 3 ml/well in GM. After 24 hours, the cells were switched to Differentiation Media (DM; DMEM with 2% horse serum (HyClone), 1% NEAA, 100 IU/ml penicillin, and 100 µg/ml streptomycin), and the media was replaced every 3 days during differentiation assays. All media components were purchased from Nacalai Tesque unless otherwise noted.

Viral constructs and production

The retroviral MSCV-IRES-EGFP vector and lentiviral FG12 vector were obtained from Addgene (#20672 and #14884, respectively). Mouse Msi2 cDNA was cloned into MSCV

vector with FLAG tag or HA tag at the N-terminus. The short hairpin RNA constructs were designed and cloned in the FG12 vector according to its instruction. The target sequences are 5'-AGTTAGATTCCAAGACGA-3' for mouse Msi2 (shMsi2) and 5'-CTGTGCCAGAGTCCTTCGATAG-3' for luciferase as a negative control (shLuc). Lentiviral short hairpin RNA (shRNA) constructs were cloned in the FG12 vector essentially as described previously. Virus was produced in 293FT cells transfected using polyethylenimine with viral constructs along with VSV-G and gag-pol. For lentivirus production Rev was also co-transfected. Viral supernatants were collected after 48 hours and 72 hours and concentrated by ultracentrifugation at 50,000 × g for 2h.

For viral transduction, cells were plated at 2×10^4 cells/ml, 3ml/dish in 60 mm dishes and culture for 24 hours. Virus and polybrene (1μg/ml) were added to the cells. After 48 hours, infection was confirmed by observing GFP fluorescence using a microscope or flow cytometry. Cells were collected and replated for further differentiation assays.

Antibodies

The following antibodies were used; for immunoprecipitation, mouse monoclonal anti-FLAG (F1804, Sigma-Aldrich), rabbit monoclonal anti-MSI2 (EP1305Y, Abcam), and normal rabbit IgG (Bethyl). For Western blotting, rabbit monoclonal anti-MSI2 (EP1305Y, Abcam), mouse monoclonal anti-HSP90 (F-8; Santa Cruz Biotech), rabbit monoclonal anti-LC3A (D50G8, Cell Signalling Technology or CST), mouse monoclonal anti-MHC (MF20, Developmental Studies Hybridoma Bank or DSHB), mouse monoclonal anti-Myogenin (F5D, DSHB), and mouse monoclonal anti-FLAG (F1804, Sigma), For immunofluorescence staining, rabbit monoclonal anti-MSI2 (EP1305Y, Abcam), mouse monoclonal anti-MHC (MF20, DSHB), rabbit monoclonal anti-LC3A (D50G8, CST), normal mouse IgG (Sigma), and normal rabbit IgG (Bethyl).

Western blotting

Protein samples were collected from cultured cells using NP40 lysis buffer (50 mM Tris-HCl pH 7.4, 150mM NaCl, 5mM EDTA, 1% NP-40) with protease inhibitor and phosphatase inhibitor (Nacalai Tesque). BCA assay (FUJIFILM Wako Chemicals) was utilized to determine protein concentration. SDS-PAGE was performed using precast gels (NW04125BOX, Thermo Fisher Scientific). Proteins were transferred to a polyvinylidene difluoride membrane using a semi-dry transfer system (iBlot2, Thermo Fisher Scientific). Chemiluminescence signal was detected using detection reagent (2332638, ATTO) by ChemiDoc MP Imaging System (Bio-Rad)

Immunofluorescence analysis

For immunofluorescence staining, C2C12 cells were plated in a 6-well plate with coverslips at the bottom of each well and differentiated as described above. After 5 or 6 days in DM, cells were fixed in 4% paraformaldehyde in PBS for 15 minutes, washed 3 times with PBS, and permeabilized in PBS with 0.5% Triton X-100 for 15 minutes. Samples were then blocked using Blocking One (Nacalai Tesque) for 30 minutes and incubated for 1 hour at room temperature (RT) with primary antibody followed by Alexa Fluor-conjugated secondary antibody and DAPI (Invitrogen). Coverslips were mounted onto slides using anti-fade mounting media containing 0.2% n-propyl gallate and fluorescence images were captured on the AxioImager Z1 (Zeiss). For differentiation and fusion indices, images were analyzed using ImageJ software. LC3 puncta were quantified using Image J with a published macro[65,66].

Flow cytometry analysis of MitoTracker Deep Red staining

Protocol was established based on published literature[67]. Cells were incubated with 10 μM carbonyl cyanide-*p*-trifluoromethoxyphenylhydrazone (FCCP) or dimethyl sulfoxide (DMSO) as a negative control for 15 min in a humidified incubator with 5% CO_2 at 37 °C. Then cells were incubated with 20 nM MitoTracker Deep Red (Thermo Fisher Scientific) or DMSO negative control for 30 min avoiding lights in a humidified incubator with 5% CO_2 at 37 °C. After incubation, cells were washed twice with PBS and then analyzed with FACSCanto II flow cytometry (BD). MitoTracker positive populations were gated based on negative control without MitoTracker addition. Mean of the APC-Area level was used as the MitoTracker staining level. The signal level of samples with the FCCP treatment were used as background level and subtracted from the signal level of samples without the FCCP treatment.

Autophagy induction during C2C12 differentiation

C2C12 cells were plated in a 6-well plate with coverslips at the bottom of each well and differentiated as described above. Twenty-four hours after differentiation induction, cells were incubated with 20 μM of Tat-Beclin1-L11S or Tat-Beclin1-D11 for 5 hours in a humidified incubator with 5% CO_2 at 37 °C. After the incubation, media were removed, and fresh DM were replenished. The cells were returned to the incubator and kept for differentiation as described above.

Realtime RT-PCR analysis

Total cellular RNAs were isolated using TRI Reagent (Sigma-Aldrich, T9424) and cDNAs were prepared from equal amounts of RNAs using Superscript IV reverse transcriptase

(Thermo Fisher Scientific). Quantitative real-time PCRs were performed using EvaGreen® qPCR Master Mix (Bio-Rad) on an StepOnePlus (Thermo Fisher Scientific). Results were normalized to the level of β-2-microglobulin. PCR primer sequences are as follows.

mB2m-F, 5’ -ACCGGCCTGTATGCTATCCAGAA-3’

mB2m-R, 5’ -AATGTGAGGCGGGTGGAACTGT-3’

mMyog-F, 5’ -CTAAAGTGGAGATCCTGCGCAGC-3’

mMyog-R, 5’ -GCAACAGACATATCCTCCACCGTG-3’

mMYH1-F, 5’ -ATGAACAGAAGCGCAACGTG-3’

mMYH1-R, 5’ -AGGCCTTGACCTTTGATTGC-3’

mMYH3-F, 5’ -TGAACAGATTGCCGAGAACG-3’

mMYH3-R, 5’ -GGAGAATCTTGGCTTCTTCGTG-3’

mMyod1-F, 5’ -TTCTTCACCACACCTCTGACA-3’

mMyod1-R, 5’ -GCCGTGAGAGTCGTCTTATCT-3’

mMYH4-F, 5’ -CACCTGGAGCGGATGAAGAAGAAC-3’

mMYH4-R, 5’ -GTCCTGCAGCCTCAGCACGTT-3’

mMAP1LC3A-F, 5’ -GACCGCTGTAAGGAGGTGC-3’

mMAP1LC3A-F, 5’ -CTTGACCAACTCGCTCATGTTA-3’

Statistical analysis

Statistical analyses were carried out using GraphPad Prism9 software (GraphPad Software Inc.). Data are shown as the mean ± the standard error of the mean, SEM.

Two-tailed unpaired Student's *t*-tests or 1-way ANOVA with Tukey's multiple comparisons tests were used to determine statistical significance. (*$p<0.05$, **$p<0.01$, ***$p<0.001$, ****$p<0.0001$).

References

1 Bentzinger CF, Wang YX, Rudnicki MA. Building Muscle: Molecular Regulation of Myogenesis. *Csh Perspect Biol* 2012; 4: a008342.

2 Kuang S, Kuroda K, Grand FL, Rudnicki MA. Asymmetric Self-Renewal and Commitment of Satellite Stem Cells in Muscle. *Cell* 2007; 129: 999–1010.

3 Chal J, Pourquié O. Making muscle: skeletal myogenesis in vivo and in vitro. *Development* 2017; 144: 2104–2122.

4 Wagers AJ, Conboy IM. Cellular and Molecular Signatures of Muscle Regeneration: Current Concepts and Controversies in Adult Myogenesis. *Cell* 2005; 122: 659–667.

5 Zammit PS. Function of the myogenic regulatory factors Myf5, MyoD, Myogenin and MRF4 in skeletal muscle, satellite cells and regenerative myogenesis. *Semin Cell Dev Biol* 2017; 72: 19–32.

6 Mizushima N, Komatsu M. Autophagy: Renovation of Cells and Tissues. *Cell* 2011; 147: 728–741.

7 Ryall JG. Metabolic reprogramming as a novel regulator of skeletal muscle development and regeneration. *Febs J* 2013; 280: 4004–4013.

8 Fortini P, Ferretti C, Iorio E, Cagnin M, Garribba L, Pietraforte D *et al.* The fine tuning of metabolism, autophagy and differentiation during in vitro myogenesis. *Cell Death Dis* 2016; 7: e2168–e2168.

9 Sin J, Andres AM, Taylor DJR, Weston T, Hiraumi Y, Stotland A *et al.* Mitophagy is required for mitochondrial biogenesis and myogenic differentiation of C2C12 myoblasts. *Autophagy* 2015; 12: 369–380.

10 Pyo J-O, Yoo S-M, Ahn H-H, Nah J, Hong S-H, Kam T-I *et al.* Overexpression of Atg5 in mice activates autophagy and extends lifespan. *Nat Commun* 2013; 4: 2300.

11 Masiero E, Agatea L, Mammucari C, Blaauw B, Loro E, Komatsu M *et al.* Autophagy Is Required to Maintain Muscle Mass. *Cell Metab* 2009; 10: 507–515.

12 He C, Bassik MC, Moresi V, Sun K, Wei Y, Zou Z *et al.* Exercise-induced BCL2-regulated autophagy is required for muscle glucose homeostasis. *Nature* 2012; 481: 511–515.

13 Sandri M. Autophagy in skeletal muscle. *Febs Lett* 2010; 584: 1411–1416.

14 Penna F, Costamagna D, Pin F, Camperi A, Fanzani A, Chiarpotto EM *et al.* Autophagic Degradation Contributes to Muscle Wasting in Cancer Cachexia. *Am J Pathology* 2013; 182: 1367–1378.

15 Aman Y, Schmauck-Medina T, Hansen M, Morimoto RI, Simon AK, Bjedov I *et al.* Autophagy in healthy aging and disease. *Nat Aging* 2021; 1: 634–650.

16 Apponi LH, Corbett AH, Pavlath GK. RNA-binding proteins and gene regulation in myogenesis. *Trends Pharmacol Sci* 2011; 32: 652–658.

17 Lunde BM, Moore C, Varani G. RNA-binding proteins: modular design for efficient function. *Nat Rev Mol Cell Bio* 2007; 8: 479–490.

18 Nikonova E, Kao S-Y, Ravichandran K, Wittner A, Spletter ML. Conserved functions of RNA-binding proteins in muscle. *Int J Biochem Cell Biology* 2019; 110: 29–49.

19 Figueroa A, Cuadrado A, Fan J, Atasoy U, Muscat GE, Muñoz-Canoves P *et al.* Role of HuR in Skeletal Myogenesis through Coordinate Regulation of Muscle Differentiation Genes. *Mol Cell Biol* 2003; 23: 4991–5004.

20 Briata P, Forcales SV, Ponassi M, Corte G, Chen C-Y, Karin M *et al.* p38-Dependent Phosphorylation of the mRNA Decay-Promoting Factor KSRP Controls the Stability of Select Myogenic Transcripts. *Mol Cell* 2005; 20: 891–903.

21 Zhao Y, Zhou J, He L, Li Y, Yuan J, Sun K *et al.* MyoD induced enhancer RNA interacts with hnRNPL to activate target gene transcription during myogenic differentiation. *Nat Commun* 2019; 10: 5787.

22 Hattori A, Buac K, Ito T. Regulation of Stem Cell Self-Renewal and Oncogenesis by RNA-Binding Proteins. *Adv Exp Med Biol* 2016; 907: 153–88.

23 Sakakibara S, Nakamura Y, Satoh H, Okano H. RNA-Binding Protein Musashi2: Developmentally Regulated Expression in Neural Precursor Cells and Subpopulations of Neurons in Mammalian CNS. *J Neurosci* 2001; 21: 8091–8107.

24 Kawahara H, Imai T, Imataka H, Tsujimoto M, Matsumoto K, Okano H. Neural RNA-binding protein Musashi1 inhibits translation initiation by competing with eIF4G for PABP. *J Cell Biology* 2008; 181: 639–653.

25 Sakakibara S, Nakamura Y, Yoshida T, Shibata S, Koike M, Takano H *et al.* RNA-binding protein Musashi family: Roles for CNS stem cells and a subpopulation of ependymal cells revealed by targeted disruption and antisense ablation. *Proc National Acad Sci* 2002; 99: 15194–15199.

26 Potten CS, Booth C, Tudor GL, Booth D, Brady G, Hurley P *et al.* Identification of a putative intestinal stem cell and early lineage marker; musashi-1. *Differentiation* 2003; 71: 28–41.

27 Wang X-Y, Penalva LO, Yuan H, Linnoila RI, Lu J, Okano H *et al.* Musashi1 regulates breast tumor cell proliferation and is a prognostic indicator of poor survival. *Mol Cancer* 2010; 9: 221–221.

28 Chiou G-Y, Yang T-W, Huang C-C, Tang C-Y, Yen J-Y, Tsai M-C *et al.* Musashi-1 promotes a cancer stem cell lineage and chemoresistance in colorectal cancer cells. *Sci Rep-uk* 2017; 7: 2172.

29 Kharas MG, Lengner CJ, Al-Shahrour F, Bullinger L, Ball B, Zaidi S *et al.* Musashi-2 regulates normal hematopoiesis and promotes aggressive myeloid leukemia. *Nat Med* 2010; 16: 903–908.

30 Park S-M, Deering RP, Lu Y, Tivnan P, Lianoglou S, Al-Shahrour F *et al.* Musashi-2 controls cell fate, lineage bias, and TGF-β signaling in HSCs. *J Exp Medicine* 2014; 211: 71–87.

31 Ito T, Kwon HY, Zimdahl B, Congdon KL, Blum J, Lento WE *et al.* Regulation of myeloid leukaemia by the cell-fate determinant Musashi. *Nature* 2010; 466: 765–768.

32 Hattori A, Tsunoda M, Konuma T, Kobayashi M, Nagy T, Glushka J *et al.* Cancer progression by reprogrammed BCAA metabolism in myeloid leukaemia. *Nature* 2017; 545: 500–504.

33 Kang M-H, Jeong KJ, Kim WY, Lee HJ, Gong G, Suh N *et al.* Musashi RNA-binding protein 2 regulates estrogen receptor 1 function in breast cancer. *Oncogene* 2017; 36: 1745–1752.

34 Kudinov AE, Deneka A, Nikonova AS, Beck TN, Ahn Y-H, Liu X *et al.* Musashi-2 (MSI2) supports TGF-β signaling and inhibits claudins to promote non-small cell lung cancer (NSCLC) metastasis. *Proc National Acad Sci* 2016; 113: 6955–6960.

35 Liang XH, Jackson S, Seaman M, Brown K, Kempkes B, Hibshoosh H *et al.* Induction of autophagy and inhibition of tumorigenesis by beclin 1. *Nature* 1999; 402: 672–676.

36 Yang K, Guo W, Ren T, Huang Y, Han Y, Zhang H *et al.* Knockdown of HMGA2 regulates the level of autophagy via interactions between MSI2 and Beclin1 to inhibit NF1-associated malignant peripheral nerve sheath tumour growth. *J Exp Clin Cancer Res Cr* 2019; 38: 185.

37 Burattini S, Ferri P, Battistelli M, Curci R, Luchetti F, Falcieri E. C2C12 murine myoblasts as a model of skeletal muscle development: morpho-functional characterization. *European J Histochem Ejh* 2004; 48: 223–33.

38 Bajaj P, Reddy B, Millet L, Wei C, Zorlutuna P, Bao G *et al.* Patterning the differentiation of C2C12 skeletal myoblasts. *Integr Biol* 2011; 3: 897–909.

39 YAFFE D, SAXEL O. Serial passaging and differentiation of myogenic cells isolated from dystrophic mouse muscle. *Nature* 1977; 270: 725–727.

40 Hasty P, Bradley A, Morris JH, Edmondson DG, Venuti JM, Olson EN *et al.* Muscle deficiency and neonatal death in mice with a targeted mutation in the myogenin gene. *Nature* 1993; 364: 501–506.

41 Davie JK, Cho J-H, Meadows E, Flynn JM, Knapp JR, Klein WH. Target gene selectivity of the myogenic basic helix–loop–helix transcription factor myogenin in embryonic muscle. *Dev Biol* 2007; 311: 650–664.

42 Wagatsuma A, Sakuma K. Mitochondria as a Potential Regulator of Myogenesis. *Sci World J* 2013; 2013: 593267.

43 Moyes CD, Mathieu-Costello OA, Tsuchiya N, Filburn C, Hansford RG. Mitochondrial biogenesis during cellular differentiation. *Am J Physiol-cell Ph* 1997; 272: C1345–C1351.

44 Quiros PM, Goyal A, Jha P, Auwerx J. Analysis of mtDNA/nDNA Ratio in Mice. *Curr Protoc Mouse Biology* 2017; 7: 47–54.

45 Malik AN, Czajka A, Cunningham P. Accurate quantification of mouse mitochondrial DNA without co-amplification of nuclear mitochondrial insertion sequences. *Mitochondrion* 2016; 29: 59–64.

46 Priault M, Salin B, Schaeffer J, Vallette FM, Rago J-P di, Martinou J-C. Impairing the bioenergetic status and the biogenesis of mitochondria triggers mitophagy in yeast. *Cell Death Differ* 2005; 12: 1613–1621.

47 Elmore SP, Qian T, Grissom SF, Lemasters JJ. The mitochondrial permeability transition initiates autophagy in rat hepatocytes. *Faseb J* 2001; 15: 1–17.

48 McMillan EM, Quadrilatero J. Autophagy is required and protects against apoptosis during myoblast differentiation. *Biochem J* 2014; 462: 267–277.

49 Zois CE, Giatromanolaki A, Sivridis E, Papaiakovou M, Kainulainen H, Koukourakis MI. “Autophagic flux” in normal mouse tissues: focus on endogenous LC3A processing. *Autophagy* 2011; 7: 1371–8.

50 Baeken MW, Weckmann K, Diefenthäler P, Schulte J, Yusifli K, Moosmann B *et al.* Novel Insights into the Cellular Localization and Regulation of the Autophagosomal Proteins LC3A, LC3B and LC3C. *Cells* 2020; 9: 2315.

51 Mohan J, Wollert T. Human ubiquitin-like proteins as central coordinators in autophagy. *Interface Focus* 2018; 8: 20180025.

52 Klionsky DJ, Abdel-Aziz AK, Abdelfatah S, Abdellatif M, Abdoli A, Abel S *et al.* Guidelines for the use and interpretation of assays for monitoring autophagy (4th edition)1. *Autophagy* 2021; 17: 1–382.

53 Shoji-Kawata S, Sumpter R, Leveno M, Campbell GR, Zou Z, Kinch L *et al.* Identification of a candidate therapeutic autophagy-inducing peptide. *Nature* 2013; 494: 201–206.

54 Blais A, Tsikitis M, Acosta-Alvear D, Sharan R, Kluger Y, Dynlacht BD. An initial blueprint for myogenic differentiation. *Gene Dev* 2005; 19: 553–569.

55 Wheeler JR, Whitney ON, Vogler TO, Nguyen ED, Pawlikowski B, Lester E *et al.* RNA-Binding Proteins Direct Myogenic Cell Fate Decisions. *Biorxiv* 2021; : 2021.03.14.435333.

56 Pala F, Girolamo DD, Mella S, Yennek S, Chatre L, Ricchetti M *et al.* Distinct metabolic states govern skeletal muscle stem cell fates during prenatal and postnatal myogenesis. *J Cell Sci* 2018; 131: jcs212977.

57 Uhlén M, Fagerberg L, Hallström BM, Lindskog C, Oksvold P, Mardinoglu A *et al.* Proteomics. Tissue-based map of the human proteome. *Sci New York N Y* 2015; 347: 1260419.

58 Human Protein Atlas proteinatlas.org. https://www.proteinatlas.org/ENSG00000153944-MSI2/tissue (accessed 26 Jul2022).

59 MacNicol MC, Cragle CE, McDaniel FK, Hardy LL, Wang Y, Arumugam K *et al.* Evasion of regulatory phosphorylation by an alternatively spliced isoform of Musashi2. *Sci Rep-uk* 2017; 7: 11503.

60 Tanida I, Ueno T, Kominami E. LC3 and Autophagy. *Methods Mol Biology Clifton N J* 2008; 445: 77–88.

61 Mammucari C, Milan G, Romanello V, Masiero E, Rudolf R, Piccolo PD *et al.* FoxO3 Controls Autophagy in Skeletal Muscle In Vivo. *Cell Metab* 2007; 6: 458–471.

62 Erbay E, Chen J. The Mammalian Target of Rapamycin Regulates C2C12 Myogenesis via a Kinase-independent Mechanism*. *J Biol Chem* 2001; 276: 36079–36082.

63 Dohl J, Passos MEP, Foldi J, Chen Y, Pithon-Curi T, Curi R *et al.* Glutamine depletion disrupts mitochondrial integrity and impairs C2C12 myoblast proliferation, differentiation, and the heat-shock response. *Nutr Res* 2020; 84: 42–52.

64 Grange RW, Meeson A, Chin E, Lau KS, Stull JT, Shelton JM *et al.* Functional and molecular adaptations in skeletal muscle of myoglobin-mutant mice. *Am J Physiol-cell Ph* 2001; 281: C1487–C1494.

65 Dagda RK, Zhu J, Kulich SM, Chu CT. Mitochondrially localized ERK2 regulates mitophagy and autophagic cell stress. *Autophagy* 2008; 4: 770–782.

66 Chu CT, Plowey ED, Dagda RK, Hickey RW, Cherra SJ, Clark RSB. Autophagy in neurite injury and neurodegeneration: in vitro and in vivo models. *Methods Enzymol* 2009; 453: 217–49.

67 Mauro-Lizcano M, Esteban-Martínez L, Seco E, Serrano-Puebla A, Garcia-Ledo L, Figueiredo-Pereira C *et al.* New method to assess mitophagy flux by flow cytometry. *Autophagy* 2015; 11: 833–843.